AD-A154 124 SPECTROSCOPIC INVESTIGATION OF MATERIALS FOR TUNABLE INFRARED LASERS(U) OKLAHOMA STATE UNIV STILLWATER DEPT OF PHYSICS R C POWELL 28 FEB 85 N00014-82-K-0109 1/1

UNCLASSIFIED F/G 20/5 NL

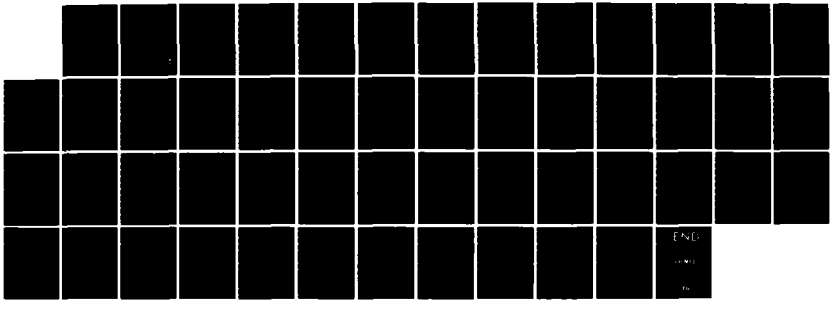

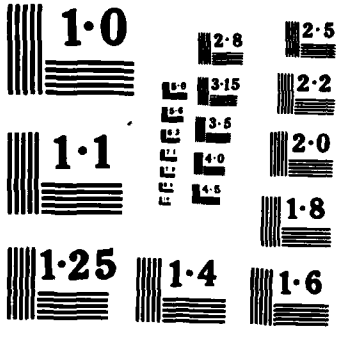
1·0
1·1
1·25
1·4
1·6
1·8
2·0
2·2
2·5
2·8
3·15
3·5
4·0
4·5

(2)

SPECTROSCOPIC INVESTIGATION OF MATERIALS FOR TUNABLE INFRARED LASERS

Richard C. Powell, Ph.D.
Principal Investigator

Department of Physics
Oklahoma State University
Stillwater, Oklahoma 74078

FINAL REPORT

Office of Naval Research
800 N. Quincy St.
Arlington, Virginia 22217

SFRC No. N00014-82-K-0109
Project No. NR 379-053/12-31-81 410

1 March 1982 - 28 February 1985

REPORT DOCUMENTATION PAGE

AD-A154124

SPECTROSCOPIC INVESTIGATION OF MATERIALS FOR TUNABLE INFRARED LASERS

Richard C. Powell

Richard C. Powell, Physics Department
Oklahoma State University
Stillwater, OK 74078

Office of Naval Research
Physics Division Office
Arlington, VA 22217

Office of Naval Research
Room 582, Federal Building
300 E. 8th St.

49

28 February 1985

Approved for public release; distribution unlimited.

Solid State Laser Materials,
4D + 5D transition metal ions, and
$RbCaF_3$: Rh^{2+} laser

The research involves the crystal growth, optical spectroscopy, and laser measurements related to the evaluation of new materials for tunable solid state lasers. The work focused on 4d and 5d transition metal ions with additional work done on 3d transition metal ions in a variety of different host crystals. Some of the results of major importance from this work are: (1) techniques were developed for the growth of crystals with 4d and 5d transition metals as dopant ions (2) techniques were developed to vary the relative amount of d-d fluorescence emission compared to charge transfer emission; and (3) tunable stimulated emission was obtained from $RbCaF_3:Rh^{2+}$ crystals.

DD FORM 1 JAN 73 1473 EDITION OF 1 NOV 65 IS OBSOLETE

SECURITY CLASSIFICATION OF THIS PAGE (When Data Entered)

ABSTRACT

This report summarizes the research done in the Department of Physics of Oklahoma State University supported by the Office of Naval Research under SFRC No. N00014-82-K-0109 from 1 March 1982 through 28 February 1985. The research involves the crystal growth, optical spectroscopy, and laser measurements related to the evaluation of new materials for tunable solid state lasers. The work focused on 4d and 5d transition metal ions with additional work done on 3d transition metal ions in a variety of different host crystals. Some of the results of major importance from this work are: (1) techniques were developed for the growth of crystals with 4d and 5d transition metals as dopant ions; (2) techniques were developed to vary the relative amount of d-d fluorescence emission compared to charge transfer emission; and (3) tunable stimulated emission was obtained from $RbCaF_3:Rh^{2+}$ crystals.

CONTENTS

I. INTRODUCTION

The goal of the research sponsored by this contract was to evaluate the potential of a variety of new materials for use as tunable solid state lasers. Currently, operating vibronic lasers are based on 3d ions such as Cr^{3+}, Ti^{3+}, Co^{2+}, and Ni^{2+} which provide tunable output in limited spectral regions. In order to increase the the spectral range covered by tunable solid state lasers, it is necessary to search for doped crystal systems based on different ions. The work proposed on this project involved investigating different 3d ions as well as some 4d and 5d transition metal ions. The research has three different aspects: crystal growth; measurement of optical spectroscopic properties; and determination of laser related parameters. The important results obtained during the three years of this contract are briefly outlined in this section and presented in detail in the remainder of the report.

I.1 Summary of Research Accomplishments

The research performed under this contract can be divided unto two thrust areas. The first is the investigation of the spectroscopic properties of 4d and 5d transition metal ions as dopants in crystalline hosts. A significant amount of the effort in this area involved developing techniques for crystal growth since little work has been done on this in the past and no commercial materials of this type are available. The spectroscopic survey of the optical properties of these materials showed that two types of optical transitions can occur: charge transfer (CT) transitions and d-d transitions. The former are strong,

allowed transitions ideal for optical pumping in the u.v. spectral region while the latter are broad bands with lifetime in the microsecond time regime which are ideal characteristics for tunable vibronic laser emission. Thermal annealing and radiation techniques were studied to enhance the amount of d-d emission compared to CT emission. Rh^{2+} was picked as an ion with a high potential for producing tunable laser emission and $RbCaF_3$ was identified as the best host crystal for this ion. Single-pass gain measurements were found to produce tunable stimulated emission with a high peak cross section in the 710 nm spectral region.

The second thrust area involved a survey of the optical spectroscopy properties of various 3d transition metal ions in different host crystals. The material showing the greatest promise as a possible laser material is Mn_2SiO_4. This is one of the few concentrated manganese systems which exhibits room temperature fluorescence.

I.2 Publications and Personnel

The personnel making major contributions to this work include the principal investigator, Richard C. Powell, the Direct of the OSU Crystal Growth Laboratory, Joel J. Martin, and several student research assistants, G.J. Quarles, R.H. Schweitzer, G.C. Gilliland, and Lin Xi. In addition, this research benefited from technical assistance in the crystal growth by C.A. Hunt, assistance in the spectroscopy measurements by G.E. Venikouas, and assistance in interpretation of spectroscopic properties by W.A. Sibley. The spectroscopic survey of 3d ions in crystals was a

joint project with Philips Research Laboratories involving G.M. Loiacono, G. Mizell, S. Colak, and W.K. Zwicker. The Na β"-alumina crystals were obtained from John Bates of Oak Ridge National Laboratory.

The work performed during the three years of this contract resulted in six publications and numerous unpublished presentations at national and international meetings. The students involved in this research have not yet completed their graduate programs, but at least one dissertation will be based on this research. Table I lists the publications from this research.

TABLE I: PUBLICATIONS

R.C. Powell, R.H. Schweitzer, J.J. Martin, G.E. Venikouas, and C.A. Hunt, "Spectroscopy of 4d and 5d Transition Metal Ions in Alkali Halide Crystals", J. Chem. Phys. 81, 1178 (1984).

R.C. Powell, G.J. Quarles, J.J. Martin, C.A. Hunt, and W.A. Sibley, "Stimulated Emission and Tunable Gain From Rh^{2+} Ions in $RbCaF_3$ Crystals", Opt. Lett. to appear in May 1985 issue.

R.C. Powell, "Recent Results on the Spectroscopy of Transition Metal Ions for Tunable Solid State Lasers", in Proceedings of the First Annual Conference on Tunable Solid State Lasers, edited by A. Pinto, A. Budgor, and P. Hammerling, (Springer-Verlag, Berlin, 1984), to be published.

R.C. Powell, J.J. Martin, R.H. Schweitzer, G.C. Gilliland, G.E. Venikouas, and C.A. Hunt, "Spectroscopic Analysis of 4d and 5d Transition Metal Ions for Tunable Solid State Laser Materials", in Proc. Int. Conf. on Lasers '83, edited by R.C. Powell (STS Press, McLean, VA, 1985), p. 157.

S. Colak, G.M. Loiacono, G. Mizell, W.K. Zwicker, and R.C. Powell, "Spectroscopic Survey of Some New Transition Metal Ion-Host Structures", in Proc. Int. Conf. on Lasers '83, edited by R.C. Powell (STS Press, McLean, VA, 1985), p. 179.

L. Xi, G.E. Venikouas, R.C. Powell, and J.B. Bates, "Spectroscopic Properties of Transition Metal Ions in Na β"-Alumina Crystals", to be published.

II. SPECTROSCOPIC PROPERTIES OF 4d AND 5d TRANSITION METAL IONS IN CRYSTALS

Figure 1 shows the d electron configurations for divalent and trivalent transition metal ions. The ions of greatest interest in this work are the divalent 4d and 5d ions. The optical properties of these ions have been studied extensively in chemical complexes but very little work has been done on these ions as substitutional impurities in crystals. To study the properties of these ions in crystals, we used both Bridgeman and Czocharlski techniques to grow single crystals of $KMgF_3$, $RbMgF_3$, $RbCaF_3$, KCl, KBr, CsBr, and $Bi_4Ge_3O_{12}$ containing various concentrations of Rh^2, Ru^{2+}, Pt^{2+}, and Ir^{2+}. In addition, a sample of $LiNbO_3$:Rh^{2+} was obtained commercially. Also, samples of Na β"-alumina crystals were obtained from Oak Ridge National Laboratories and Rh^{2+} diffused into the material. Results obtained on this last type of material are described in Sec. III.1. Although the types of host crystals used in this study were easy to grow in large sizes and with good optical quality, substituting the doping ions into the host lattice proved to be quite difficult. The chloride starting materials decompose at such low temperatures that the active ions would not go into the melt. Maintaining a uniform distribution and stable valance state was also a major problem. The crystal growth problems were solved by using double enclosed crucibles.

Figure 2 shows the charge transfer absorption bands for some of these materials. The d-d absorption bands are too weak to be seen. Nitrogen laser emission is ideally suited to pump these materials in the CT bands as shown by the arrow in the figure.

DIVALENT & TRIVALENT TRANSITION METAL IONS

$3d^{1(9)}$	$3d^{2(8)}$	$3d^{3(7)}$	$3d^{4(6)}$	$3d^{5}$
Sc^{2+}	V^{3+}	V^{2+}	Mn^{3+}	Mn^{2+}
Ti^{3+}	(Ni^{2+})	Cr^{3+}	(Fe^{2+})	Fe^{3+}
(Cu^{2+})	Ti^{2+}	(Co^{2+})	(Co^{3+})	
		(Ni^{3+})	Cr^{2+}	

$4d^{1(9)}$	$4d^{2(8)}$	$4d^{3(7)}$	$4d^{4(6)}$	$4d^{5}$
Y^{2+}	(Pd^{2+})	(Rh^{2+})	(Ru^{2+})	Ru^{3+}
Zr^{3+}		(Pd^{3+})	(Rh^{3+})	
(Cd^{3+})				

$5d^{1(9)}$	$5d^{2(8)}$	$5d^{3(7)}$	$5d^{4(6)}$	$5d^{5}$
La^{2+}	(Pt^{2+})	(Ir^{2+})	Re^{3+}	Re^{2+}
		(Pt^{3+})	(Os^{2+})	Os^{3+}
			(Ir^{3+})	

Fig. 1 d electron configurations for divalent and trivalent transition metal ions.

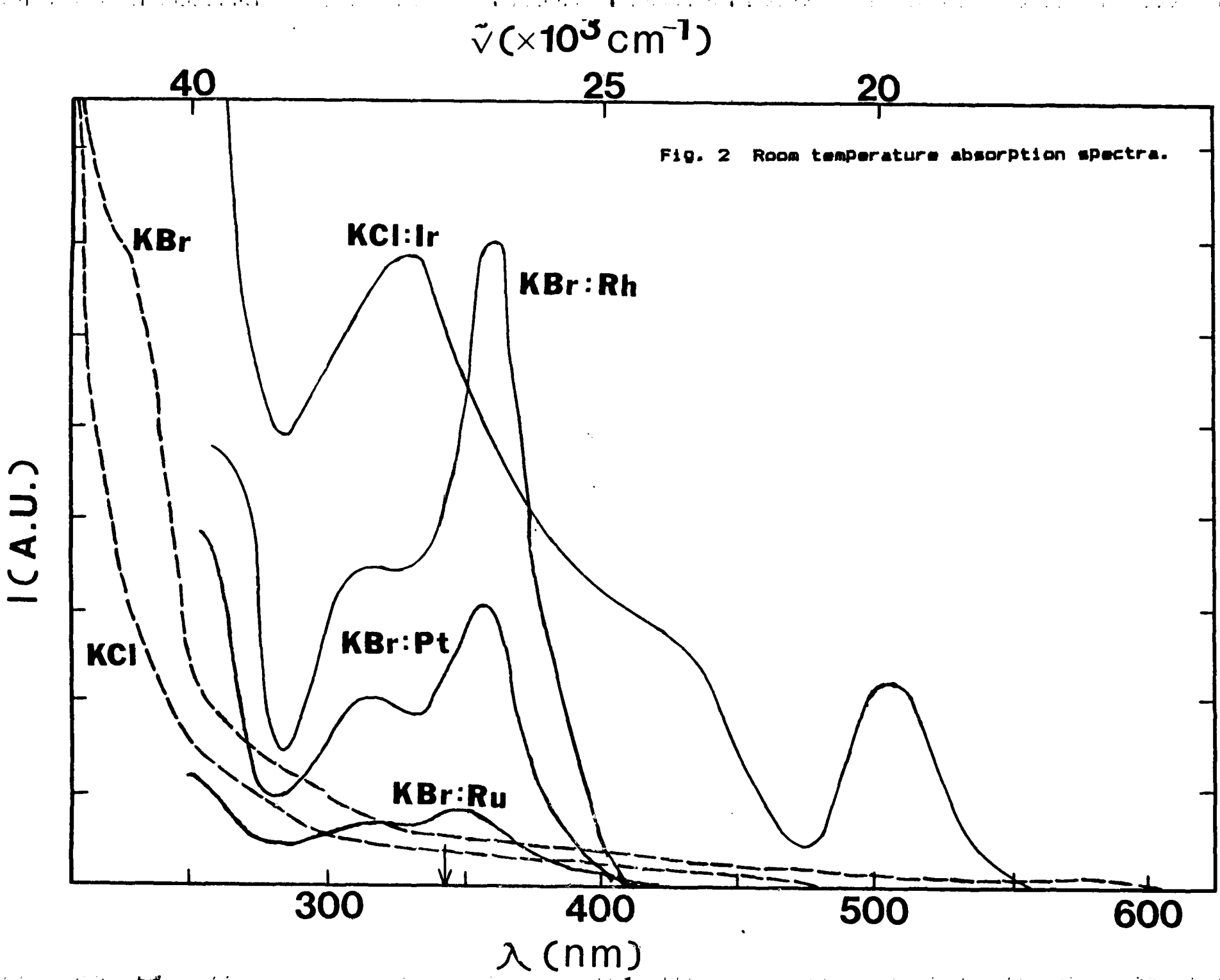

Fig. 2 Room temperature absorption spectra.

The following two manuscripts describe the results obtained on studying the optical properties 4d and 5d transition metal ions in crystals. These results are important because they provide the first description of the spectral features of these types of materials, show how to enhance d-d emission through thermal and radiation treatments, and demonstrate stimulated emission and tunable gain from one of these materials.

Spectroscopy of 4*d* and 5*d* transition metal ions in alkali halide crystals

Richard C. Powell, Robert H. Schweitzer, Joel J. Martin, George E. Venikouas, and Charles A. Hunt
Physics Department, Oklahoma State University, Stillwater, Oklahoma 74078

(Received 6 January 1984; accepted 2 April 1984)

The fluorescence spectra and lifetimes of divalent Rh, Ru, Pt, and Ir ions in alkali halide crystals are measured using pulsed nitrogen laser excitation. Emission from both the charge transfer states and the excited *d* levels is observed. Changes in the relative intensities and lifetimes are monitored as a function of temperature, annealing, and radiation treatment. The results are interpreted in terms of the possible application of these materials for tunable solid state lasers.

I. INTRODUCTION

There is currently a significant amount of interest in identifying new materials for use as tunable solid state lasers. Thus far most of the research and development in this area has involved either 3*d* transition metal ions such as Cr, Co, and Ni in oxide hosts or color centers in alkali halide and oxide crystals. Another class of ions which may be useful in this application is the 4*d* and 5*d* transition metals and research is underway to survey the spectroscopic properties of these ions in different types of host crystals. This paper describes the results obtained on crystals of KCl:Ru^{2+}, KBr:Rh^{2+}, KCl:Ir^{2+}, and KBr:Pt^{2+}. Fluorescence intensities and lifetimes were measured as a function of temperature, annealing, and radiation treatment. The results are interpreted in terms of emission from both charge transfer states and excited *d* levels.

Extensive literature exists on the spectroscopic properties of 3*d* and 4*d* transition metal ions in chemical complexes.[1–4] Systematic studies have been performed on the spectral changes that occur with changes in the ligands and the structure of the chemical complex. Emission has been observed from charge transfer states, spin-allowed transitions from excited *d* levels, and spin-forbidden transitions from excited *d* levels. The two series of ions exhibit a variety of broad emission bands throughout the visible region of the spectrum. However very little work has been done on these ions as dopants in single crystals.[5–7] The goal of this work is to begin to understand the properties of 4*d* and 5*d* transition metal ions in crystals and to develop techniques for enhancing *d* level emission compared to charge transfer emission.

A. Samples

The crystals used in this project were grown by the Czochralski method of pulling from the melt. All growth was carried out in a dry nitrogen atmosphere in an internally heated furnace. Fisher Scientific reagent grade KBr and KCl were used for the host starting materials. The $PtCl_2$ (99.9%), $RhCl_3$ (99.9%), $IrCl_3$ (99.95%), and $RuCl_3$ (99.9%) anhydrous dopants were obtained from the Gallard–Schlesinger Co. The melts were contained in high purity alumina crucibles. After the crystals were grown, they were slowly cooled to room temperature over a 16 h period. Samples were cleaved from the boule perpendicualr to the growth axis so as to ensure uniform doping.

Example crystals were analyzed with an EDXA attachment on an electron microscope to determine the concentration and distribution of the doping ions and to detect the presence of other impurities. In addition, electron paramagnetic resonance measurements were made on example samples to determine the valence of the optically active ions. The results of these measurements indicate that the dopant ions are distributed uniformly at concentrations of around 200 ppm. No significant amount of other optically active impurities or other valence states of the dopant ions were detected.

The ions of interest in this study are $Rh^{2+}(4d^7)$, $Ru^{2+}(4d^6)$, $Pt^{2+}(5d^8)$, and $Ir^{2+}(5d^7)$. Partial crystal field energy level diagrams for these d^n electron configurations[8] are shown in Fig. 1. The figure is restricted to the lowest sets of energy levels in the strong crystal field region since this area contains the transitions of interest in interpreting the observed spectra. For each case there is a low lying set of excited states which can give rise to spin-forbidden transitions to the ground state and a higher set of states which can produce spin-allowed transitions to the ground state. Interactions between the transition metal ion and its ligands result in charge transfer states which lie at higher energies with respect to the *d* levels shown in the figure.

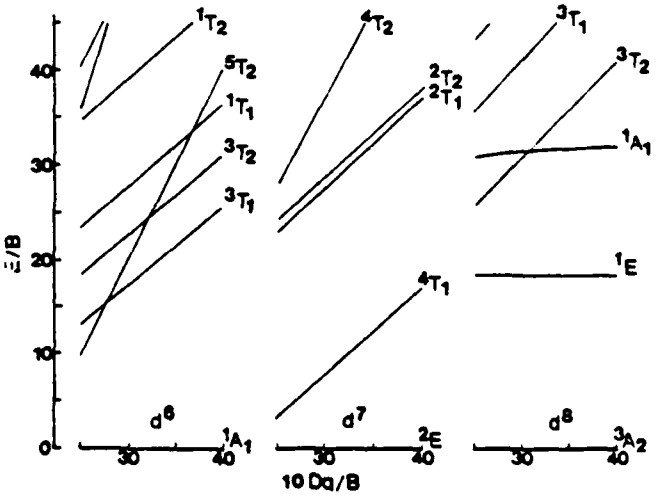

FIG. 1. Portions of crystal field crystal field energy level diagrams for d^6, d^7, and d^8 ions in octahedral environments.

B. Experimental apparatus

Measurements of the fluorescence spectra and lifetimes were made using a pulsed nitrogen laser for excitation. This provided a pump pulse at 337.1 nm which was about 10 ns in duration and 1 Å in half-width. The samples were mounted in a cryogenic refrigerator capable of controlling the temperature between about 10 K and room temperature. The fluorescence was focused onto the entrance slit of a 1 m monochromator with the slits set for 20 Å resolution. The signal was detected by a cooled RCA C31034 photomultiplier tube and analyzed by a boxcar integrator before being displayed on a strip chart recorder.

To measure lifetimes the window of the boxcar was set in the scanning mode with a time resolution of about 50 ns. The fluorescence spectra were recorded at fixed times after the excitation pulse. Both fast and slow emission bands were observed in these materials and this time-resolved fluorescence technique can be used to emphasize either one of these two types of emissions. Examples of the observed spectra are presented in the following section. Because of the large difference in lifetimes, it is difficult to show both types of emissions on the same spectra. To overcome this problem, the spectra shown in the figures were obtained at 50 μs after the laser pulses using a 1 MΩ load resistance which distorts the timing of the spectra and allows both types of bands to be easily seen. Thus the absolute magnitudes of the spectral bands in these figures are not meaningful but the relative changes in intensities between samples or with different experimental conditions are accurate.

In the absorption spectra of these samples, it was not possible to detect any bands due to the doping ions. Only the normal absorption edges of the host crystals near 250 nm were observed. Excitation spectra taken with a xenon lamp and 1/4 m monochromator showed the major absorption in all of the samples to occur as a triple peaked band between about 280 and 400 nm. The Ir doped sample exhibited additional excitation bands in the 500 to 600 nm region of the spectrum.

A 2 MeV van de Graaff accelerator was used for radiation treatment of the samples.

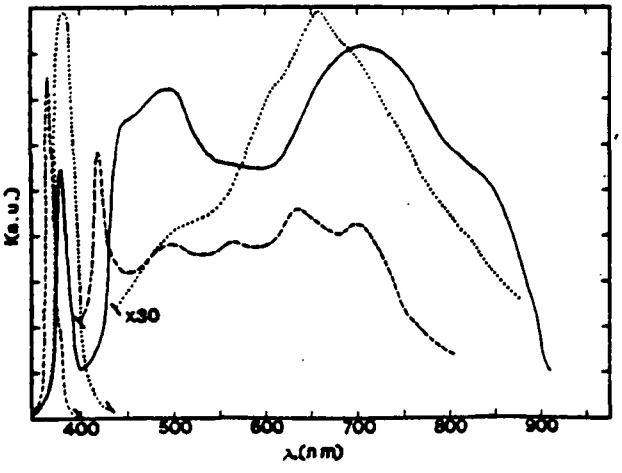

FIG. 2. Fluorescence spectra of KBr:Pt after pulsed N_2 laser excitation. — 300 K, freshly cleaved samples; - - -10 K freshly cleaved sample; -- 300 K aged sample. (All samples unirradiated.)

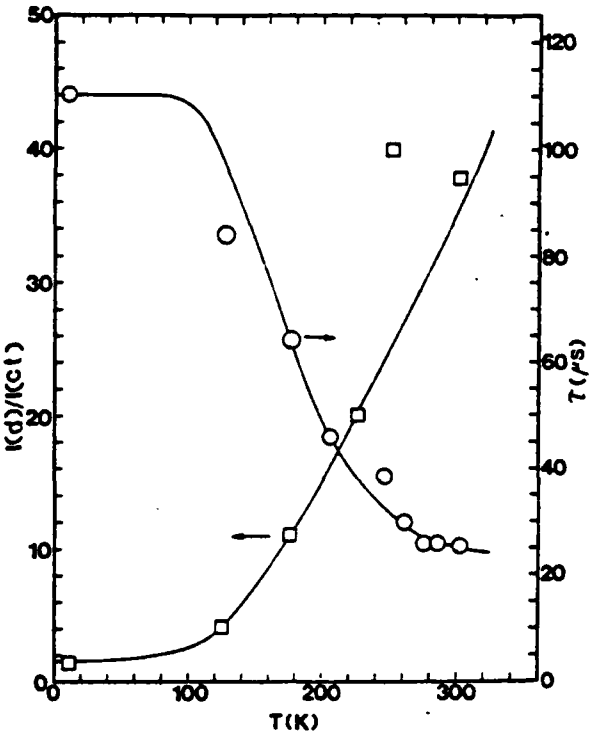

FIG. 3. Temperature dependences of the fluorescence lifetime of the *d* emission and the ratios of the integrated intensities of the *d* and charge transfer emission for KBr:Pt. See the text for explanation of the theoretical lines.

II. EXPERIMENTAL RESULTS

A. KBR:Pt^{2+}

Figure 2 shows the fluorescence spectra obtained for Pt^{2+} in KBr crystals at room temperature and 10.2 K for a freshly cleaved surface and at room temperature for an aged surface. There are two distinct spectral regions: the relatively narrow band at 380 nm and the broad, structured band between about 425 and 850 nm. The former has a fluorescence lifetime of less than 20 ns independent of temperature and is attributed to emission from the charge transfer state, whereas the latter band has a temperature dependent lifetime in the microsecond time regime and is attributed to transitions between triplet *d* levels. The structure in the broadband shows the presence of several different *d* to *d* transitions split into two major bands. The relative intensities of the fluorescence band show that the fraction of the total emission occurring in the *d* to *d* transitions decreases with respect to that originating from the charge transfer state as the sample surface ages. At the same time the lower energy *d* emission band increases relative to the higher energy *d* emission band. These relative intensities also vary with temperature with the *d* to *d* emission relative to the charge transfer emission decreasing as temperature is lowered.

Figure 3 shows the temperature dependencies of the emission intensities and lifetime for this sample. The ratio of the total emission from the *d* levels to that of the charge transfer level increases with temperature reaching a maximum at 250 K. Although both major *d* emission bands increase in intensity with temperature up to 250 K, the higher energy band increases more rapidly. Above this temperature the higher energy band decreases while the low energy band

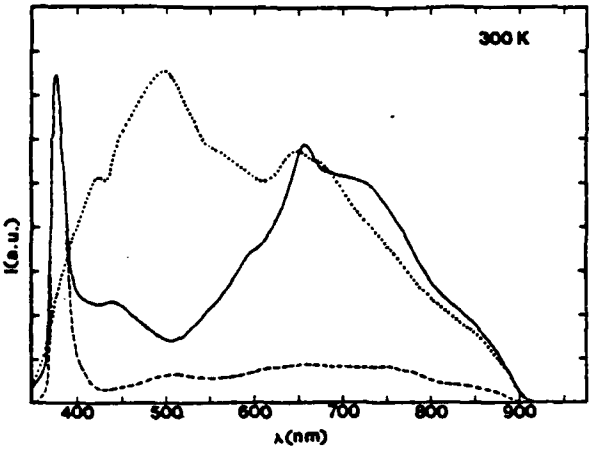

FIG. 4. Fluorescence spectra of KBr:Rh at 300 K after pulsed N_2 laser excitation. - - - untreated sample; —irradiated sample; · · · annealed sample.

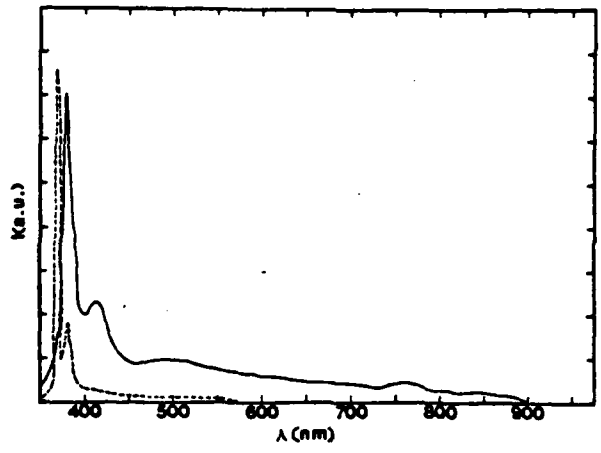

FIG. 6. Fluorescence spectra of KCl:Ir after pulsed N_2 laser excitation at 10 K(- - -) and room temperature (—) of a freshly cleaved, unirradiated sample.

continues to increase with temperature. The solid lines in the figure represent the best fits to the data using the model discussed below.

B. KBr:Rh^{2+}

Figure 4 shows the emission spectra of KBr:Rh^{2+} at room temperature for an as-grown sample, a crystal that has been exposed to a radiation dose of 10^5 rad of electrons, and a sample that was annealed by heating to 600 °C and fast cooling on a copper block. Again both charge transfer and spin allowed doublet *d* emission bands are observed. Both radiation and heat treatment enhance the *d* emission with respect to the charge transfer emission. The former treatment tends to preferentially increase the lower energy *d* band while the latter preferentially increases the higher energy *d* band.

Figure 5 shows the temperature dependences of the relative intensities and fluorescence lifetime of the *d* emission. The trends are similar to those discussed above for Pt except that the intensity ratios show a more pronounced maximum near 250 K. The solid line represents the theoretical fit discussed below while the dashed line simply shows the general trend of the intensity ratios. Again the lifetime of the charge transfer emission is less than 20 ns and no change with temperature could be observed within the time resolution of our instrumentation.

C. KCl:Ir^{2+}

Figures 6 and 7 show the spectra and temperature de-

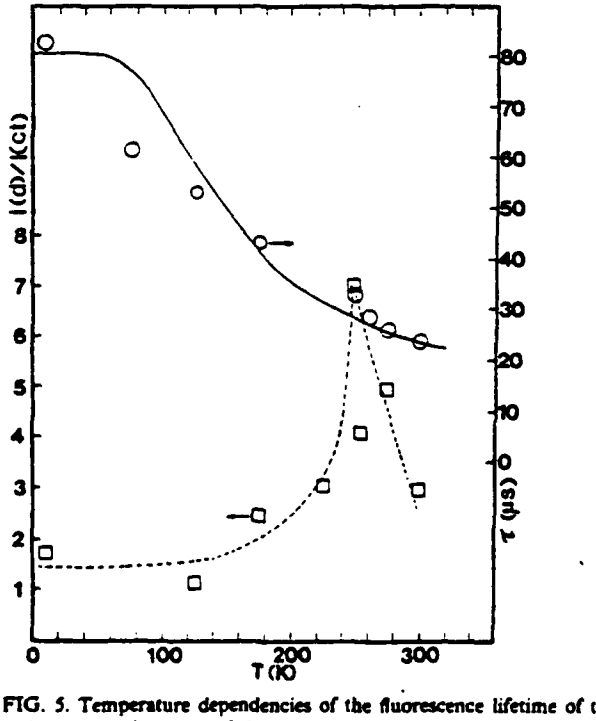

FIG. 5. Temperature dependencies of the fluorescence lifetime of the *d* emission and the ratios of the integrated intensities of the *d* and charge transfer emissions for KBr:Rh. See the text for explanation of the theoretical curve.

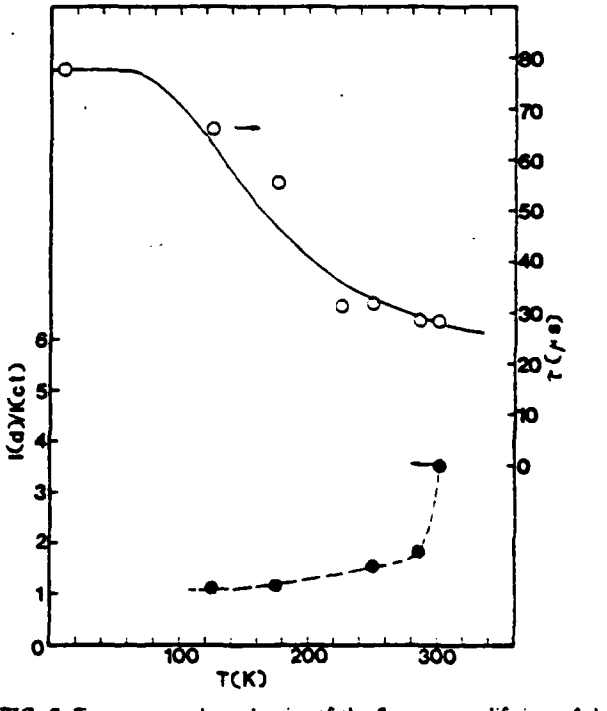

FIG. 7. Temperature dependencies of the fluorescence lifetime of the *d* emission and the ratios of the integrated intensities of the *d* and charge transfer emissions for KCl:Ir. See the text for explanation of the theoretical curve.

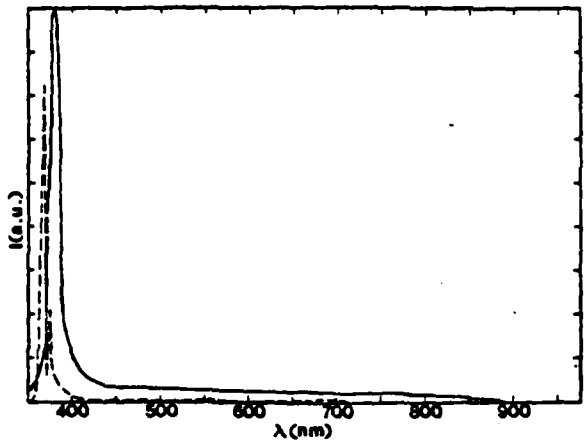

FIG. 8. Fluroescence spectra of KCl:Ru after pulsed N_2 laser excitation at 10 K (- - -) and room temperature (—) of a freshly cleaved, unirradiated sample.

pendencies of the lifetimes and relative intensities for KCl:Ir^{2+} crystals. The results are similar to those observed in the other samples except that the *d* emission intensity is much weaker in comparison to the charge transfer bands.

D. KCl:Ru^{2+}

Figures 8 and 9 show the results obtained for KCl:Ru^{2+} crystals. This case shows the weakest *d* emission compared to the charge transfer emission at room temperature. Unlike the other samples, this material shows a slight increase in the intensity ratios as temperature is lowered.

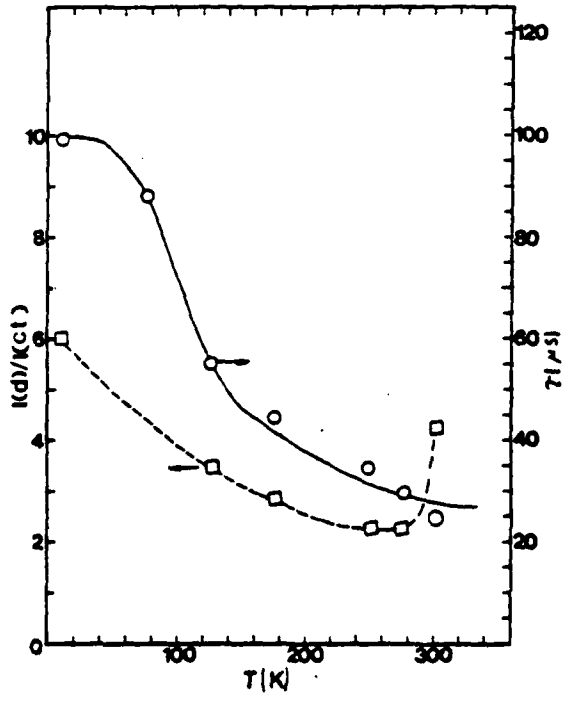

FIG. 9. Temperature dependences of the fluorescence lifetime of the *d* emission and the ratios of the integrated intensities of the *d* and charge transfer emission for KCl:Ru. See the text for explanation the theoretical curve.

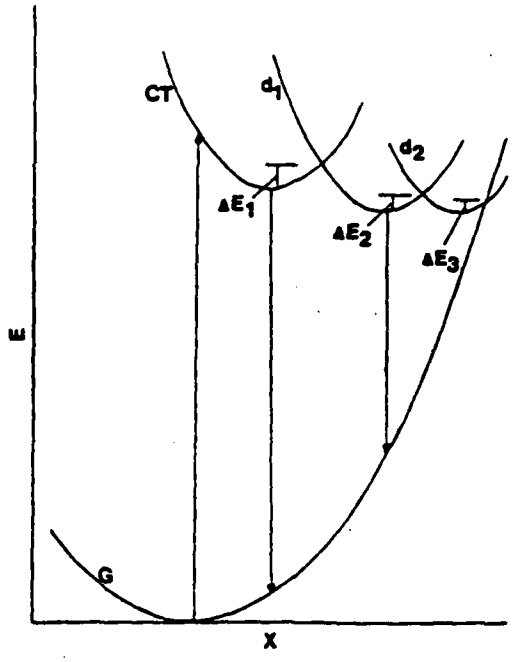

FIG. 10. Simplified single configuration coordinate model for interpreting the experimental results.

III. INTERPRETATION

The spectroscopic results described in the last section are quite complex and obviously involve dynamic interactions among several different types of charge transfer and *d* levels. The exact details of these interactions can not be determined without more extensive experimental results but the general spectroscopic features can be interpreted in terms of the simplified single configuration coordinate model shown in Fig. 10. The manifold of crystal field split charge transfer states are represented by one potential curve and the system of *d* levels is represented by one ground state and two excited state potential curves. At low temperatures the absorption transition is followed by radiationless relaxation to the bottom of the charge transfer potential well. The majority of the emission occurs from this relaxed state. As temperature is raised, higher energy vibrational levels of the charge transfer state are occupied and when an energy ΔE_1 is reached, crossover occurs to the higher energy *d* level. Transfer to the lower *d* level occurs at a temperature consistent with ΔE_2 and fluorescence emission occurs from the bottom of both the *d* potential wells. At temperatures above that consistent with an energy ΔE_3 radiationless decay to the ground state occurs. The temperature dependencies of the relative intensities and lifetimes depend on the energies ΔE_1, ΔE_2, and ΔE_3.

The intensity of the fluorescence emission from each level is proportional to the concentration of ions in the level, n_i. Representing all of the charge transfer states by one level and all of the excited *d* states by one level, the rate equations of the excited state populations are

$$dn_{ct}/dt = W_{ct} - \tau_{ct}^{-1} n_{ct} - \beta n_{ct},$$
$$dn_d/dt = W_d - \tau_d^{-1} n_d + \beta n_{ct}, \quad (1)$$

where the W_i represent the pumping rates, the τ_i are the fluorescence lifetimes, and β is the radiationless relaxation rate between the two sets of levels. These equations can be solved simultaneously and the resulting expressions for the time dependences of the excited state populations are directly proportional to the measured fluorescence intensities. This procedure provides equations for fitting the experimental data on the temperature variations of the fluorescence lifetimes and relative intensities.

The temperature dependencies of the ratios of fluorescence intensities at a specific time after the excitation pulse can be expressed as

$$I_d/I_{ct} = A + B\exp(-\Delta E_1/kT). \tag{2}$$

The temperature independent coefficients A and B contain factors describing the ratios of the initial pumping rates and the radiative decay rates of the two types of levels as well as a correction factor for the detection sensitivity in the different spectral ranges of the two types of emissions and an exponential time factor. The exponential temperature dependence comes from expressing the parameter β as the ratio of the rates of absorption and emission of phonons coupling the charge transfer and d states.

The solid line in Fig. 3 represents the best fit to the temperature dependent intensity data for KBr:Pt using Eq. (2) and treating A, B, and ΔE_1 as adjustable parameters. This fit was obtained for $A = 1.69$, $B = 240$, and $\Delta E_1 = 398$ cm^{-1}. The simple model used here can not explain the peak in the intensity ratios at 250 K which is associated with the redistribution of energy among the several different ct and d levels which are present in the sample.

Similar good fits to the observed temperature dependences of the intensity ratios could not be obtained for the other samples. In the case of KBr:Rh the peak at 250 K is too dominant to allow the simplified model to be a good approximation. For KCl:Ir the strong increase with temperature begins to occur near 300 K. This indicates a higher value of ΔE_1 but the measurements do not extend to high enough temperatures to obtain an accurate theoretical fit. The temperature dependence of the intensity ratios for KCl:Ru is the opposite of that predicted by the simple model used here which is probably due to redistribution of the energy among different types of charge transfer states with different radiative emission rates. Some evidence for this can be seen in the spectra shown in Fig. 8.

The temperature dependencies of the fluorescence lifetimes of the d emission bands can be interpreted by a model assuming the presence of two d levels with different intrinsic decay times τ_{LT} and τ_{HT} separated by an energy barrier, ΔE_2, and connected by efficient radiationless processes so that the populations of the levels are in thermal equilibrium. For this situation the observed fluorescence decay time will be the weighted combination of the two intrinsic decay times

$$\tau = \{1 + G\exp(-\Delta E_2/kT)\}/\{(1/\tau_{LT}) + (1/\tau_{HT})G\exp(\Delta E_2/kT)\}, \tag{3}$$

where G is the ratio of the degeneracies of the two states. This equation gives a reasonably good fit to the lifetime data for all four samples as shown in Figs. 3, 5, 7, and 9. The solid lines are obtained treating G, ΔE_2, and the two intrinsic lifetimes as adjustable parameters. The numerical results for these parameters are listed in Table I. The values obtained are physically reasonable except for the value of $G = 50$ for KBr:Pt. This high value indicates that the structure of the d manifold of levels is more complex than the simple model employed here.

The changes in sample properties after various types of treatments are associated with the defect structure of the material. When divalent ions are incorporated in alkali halide crystals, charge compensation is necessary. Usually this takes the form of alkali ion vacancies which are not necessarily located close to the dopant ions. These defects are mobile and aging, annealing, and radiation treatments can cause the formation and redistribution of defect centers. The spectral changes observed for the samples studied here due to these types of treatments can be attributed to the effects of the interaction of the dopant ion with near neighbor lattice defects. The position and shape of the charge transfer potential well is especially sensitive to changes in the ligand structure in the environment of the transition metal ion. Shifting this potential well can significantly change the efficiency of radiationless transfer from the charge transfer state to the d levels. The spectra shown in Figs. 3 and 5 indicate that local charge compensation greatly enhances the crossover to the d levels. Similar results were observed on other samples such as KCl:Ru. However, no significant changes in the spectrum were observed in a sample of $KMgF_3$:Rh after annealing. This is due to the fact that the defect mobility in $KMgF_3$ crystals is greatly reduced compared to alkali halides.

TABLE I. Spectroscopic parameters.

Parameter	Crystal KCl:Ru ($4d^6$)	KBr:Rh ($4d^7$)	KCl:Ir ($5d^7$)	KBr:Pt ($5d^6$)
λ_p (nm)	588	650	636	660
$\Delta\lambda$ (nm)	268	270	226	216
τ_f (μs)	46	25	35	23
σ_p (10^{-21} cm^2)	1.16	2.10	2.50	3.27
ΔE_2 (cm^{-1})	275	355	350	700
τ_{LT} (μs)	99	80	78	110
τ_{HT} (μs)	19	13	12.4	13.7
G	5	3.75	2.5	50

IV. DISCUSSION AND CONCLUSIONS

Table I summarizes the spectral properties of the four samples studied in this work. The results indicate that the energy levels and dynamics of 4*d* and 5*d* transition metal ions in alkali halide crystals are quite complex. The spectra shown in Figs. 2, 4, 6, and 8 show structure indicating the existence of several different types of excited state levels and the significant changes observed with variations in temperature or different types of sample treatment indicate that the population dynamics of these levels is extremely sensitive to the local environment of the dopant ion and to lattice vibrations. The simplified configuration coordinate model proposed here is useful in interpreting some of the general spectral properties but additional, systematic studies are necessary to gain a complete understanding of these materials.

The identification of the peaks appearing in the near UV spectral region as being due to charge transfer transitions and the peaks in the visible spectral region as being due to spin-allowed *d–d* transitions is somewhat arbitrary. However these assignments are consistent with the observed strengths of these peaks in absorption and with their fluorescence lifetimes as compared to the values of these parameters generally measured for these different types of transitions. In addition, the overall spectral properties of these materials are similar to those observed for these ions in chemical complexes[1–4] where much work has been done to unambiguously identify the bands belonging to charge transfer and *d–d* transitions. A similar definitive assignment for the materials investigated here must await further experiments to provide conclusive information about the local structure and ligand interactions in these crystalline environments. Since the materials investigated here contain lattice vacancies necessary for charge compensation of the doping ions, and since radiation treatment is used to alter the spectral characteristics of the samples, it is important to note that the spectral properties of color centers in these alkali halide host crystals are well known,[9] and none of the reported spectral features are consistent with color center transitions.

The general location of the charge transfer bands is approximately the same for both of the 4*d* and both of the 5*d* transition metal ions in the two types of alkali halide host crystals. However, the exact peak positions, widths, and structure of these bands are different for each sample. For example, the ct bands in both KCl samples appear as two extremely narrow transitions, whereas in both KBr samples they are broader, single transitions. This demonstrates the general similarity of the host–impurity ion systems and the effects of different ligands on the spectral details. These results are again similar to those obtained on chemical complexes of these ions.[1–4]

For a detailed spectral analysis of these 4*d* and 5*d* transition metal ions in solids, it would be desirable to obtain specific information on the local crystal field at the site of the ions. In this case it is difficult to do for two reasons: the very weak *d–d* absorption transitions and the lack of complete crystal field diagrams for these types of ions. The Sugano–Tanabe diagrams such as those shown in Fig. 1 work well for ions of the 3*d* transition metal series but the increased spin-orbit interaction causes a breakdown of the Russell–Saunders coupling for 4*d* and 5*d* ions. Although some work has been done in treating these types of ions in an intermediate coupling scheme,[10] complete crystal field energy level diagrams are not yet available for d^6, d^7, and d^8 ions. Therefore the diagrams in Fig. 1 are used to estimate the values of Dq but the results should be taken as only rough approximations to be used for comparative purposes. Considering that the broad, overlapping bands give only approximate values for the energy level positions, that the Stokes shifts of the *d* levels between absorption and emission are unknown, and that local charge compensation produces a strong deviation from an octahedral crystal field, it is not possible at the present time to do a more exact theoretical analysis of the specific systems investigated here.

Only the structure of the spectra of Pt^{2+} and Rh^{2+} in Figs. 2 and 4, respectively, is detailed enough to use in crystal field analysis. The free ion Racah parameters B for these ions are 699 cm^{-1} for Pt^{2+} and either 438 or 458 cm^{-1} for Rh^{2+} depending on the wave functions used in the calculations.[10] The structure in the spectra of Fig. 2 can be interpreted as due to transitions from the components of the $^3T_2$ and $^3T_1$ split by spin-orbit interaction and low symmetry contributions to the crystal field. The average value of the three lowest energy peak positions can be used as an estimate of the position of the $^3T_2$ energy level in an octahedral field. Dividing this energy by B provides a value for E/B to use the crystal field diagram for d^8 ions shown in Fig. 1. This leads to a cubic crystal field parameter of $Dq = 1188$ cm^{-1}. A similar analysis relating the structure of the Rh^{2+} spectra to transitions from the split components of the $^2T_1$ and $^2T_2$ levels results in a value of $Dq = 1230$ cm^{-1}. The only published value of Dq for Rh^{2+} is 1600 cm^{-1} in $ZnWO_4$ crystals.[11] This is consistent with the lower bound, Stokes shifted value of Dq given above. More acurate crystal field analysis of these materials requires samples with higher concentrations of doping ions so that the positions of *d–d* absorption transitions can be accurately determined.

The broad *d* emission bands for these materials are attractive possibilities for tunable laser applications. One critical parameter for this consideration is the peak emission cross section given by

$$\sigma_p = \{0.02\lambda_p^2\eta\}/\{n^2\Delta\nu\tau_f\}, \tag{4}$$

where λ_p is the peak wavelength of the emission band and $\Delta\nu$ is its frequency half-width. η is the quantum efficiency. The latter quantity is difficult to determine accurately since no temperature dependent intensity quenching is observed in the temperature region studied. In calculating σ_p a value of 0.5 was used for η which should be a good approximation in comparison to previous results on chemical complexes of these ions. The values obtained for the cross sections are listed in Table I and are all of the order of 10^{-21} cm^{-1} which is similar to σ_p for 3*d* ion transition metal vibronic laser materials. The lifetimes of the order of tens of microseconds indicate that fast laser pumping would be better than flashlamp pumping of these materials. This type of pumping should be very efficient since these materials have strong charge transfer absorption band coincident with the N_2 laser

wavelength. To test these materials as lasers, crystal growth techniques are being developed to incorporate an order of magnitude higher concentration of dopant ions in the host crystals. No evidence for emission from the low energy states with spin forbidden transitions was observed in these host crystals. There is some evidence that intersytem crossing to these levels is more efficient in oxide crystal hosts[5] and samples of this type are under preparation. These transitions should have millisecond lifetimes and be better suited for flashlamp pumped laser applications.

In conclusion, this work demonstrates the existence of both charge transfer and *d* level fluorescence emission from 4*d* and 5*d* transition metal ions in alkali halide crystals. It also shows how the *d* emission can be enhanced through thermal or radiation treatments resulting in broad fluorescence bands thoughout the visible region of the spectrum. These materials may be useful in tunable laser applications if samples can be prepared with high enough levels of doping.

ACKNOWLEDGMENTS

This research was supported by the Office of Naval Research and the U.S. Army Research Office. The authors express their appreciation to L. E. Halliburton, Z. F. Al Shaieb, and G. D. Gilliland for technical assistance in this work and to W. A. Sibley for helpful discussions concerning the interpretation of the results.

[1]G. A. Crosby, W. G. Perkins, and D. M. Klassen, J. Chem. Phys. 43, 1498 (1965); K. W. Hipps, G. A. Merrell, and G. A. Crosby, J. Phys. Chem. 80, 2232 (1976); J. N. Demas and G. A. Crosby, J. Am. Chem. Soc. 92, 7262 (1970); 93, 2841 (1971); W. A. Fordyce and G. A. Crosby, *ibid.* 21, 1455 (1982).

[2]R. J. Watts and G. A. Crosby, J. Am. Chem. Soc. 94, 2606 (1972); T. R. Thomas, R. J. Watts, and G. A. Crosby, J. Chem. Phys. 59, 2123 (1973); R. J. Watts and D. Missimer, J. Am. Chem. Soc. 100, 5350 (1978).

[3]W. Halper and M. K. DeArmond, J. Lumin. 5, 225 (1972).

[4]F. Diomedi Camassei, L. Ancarani-Rossiello, and F. Castelli, J. Lumin. 8, 71 (1973).

[5]G. Blasse and A. Bril, J. Electrochem. Soc. 114, 1306 (1967).

[6]C. D. Flint and A. G. Poulusz, Mol. Phys. 41, 907 (1980).

[7]W. Holzapfel, H. Yersin, and G. Gliemann, J. Chem. Phys. 74, 2124 (1981).

[8]S. Sugano, Y. Tanabe, and H. Kamimura, *Multiplets of Transition-Metal Ions in Crystals* (Academic, New York, 1970).

[9]A. E. Hughes, D. Pooley, H. U. Rahman, and W. A. Runciman, United Kingdom Atomic Energy Research Establishment Report R5604, 1967.

[10]A. S. Chakravarty, *Introduction to the Magnetic Properties of Solids* (Wiley, New York, 1980); see also S. Basu and A. S. Chakravarty, Phys. Rev. B 26, 4327 (1982); 27, 6495 (1983); V. P. Desai and A. S. Chakravarty, Proc. Nucl. Phys. Solid State Phys. Symp. 14c, 563 (1972).

[11]M. G. Townsend, J. Chem. Phys. 41, 3149 (1964).

STIMULATED EMISSION AND TUNABLE GAIN FROM Rh^{2+} IONS IN $RbCaF_3$ CRYSTALS

Richard C. Powell, Greg J. Quarles, Joel J. Martin,
Charles A. Hunt and William A. Sibley
Department of Physics, Oklahoma State University,
Stillwater, OK 74078

Stimulated emission was detected in $RbCaF_3:Rh^{2+}$ crystals through the observation of power dependent shortening of the fluorescence lifetime and narrowing of the emission band with a distinct threshold. In addition, single pass gain was observed to be tunable between about 700 and 720 nm.

Tunable solid state lasers are potentially important for various electro-optic systems applications. This has generated significant interest in developing new vibronic laser materials.[1] Most research in this area has centered around 3d transition metal ions.[2-7] However, it was shown recently that the spectroscopic properties of 4d and 5d transition metal ions make them possible candidates for vibronic lasers.[8] We report here the first tunable laser action in materials of this type using $RbCaF_3:Rh^{2+}$ as an example.

The Rh-doped $RbCaF_3$ crystal was grown by the Bridgman method in the OSU Crystal Growth Laboratory. Stoichiometric amounts of "Optran zone refined" RbF and CaF_2, and 0.1 at. % of 99.9 % $RhCl_3$ were loaded in the platinum crucible. The growth run was done in a gettered Ar atmosphere. The host crystal has a cubic perovskite structure at room temperature[9] and the Rh^{2+} ions substitute for the Ca^{2+} ions with no charge compensation or size mismatch problems. Thus they occupy a site with O_h symmetry and six-fold coordination of the F^- ligands. The sample used for this work was cleaved from the boule along (100) planes and was about 1.0 cm in diameter and 0.45 cm thick. It contained a high density of scattering centers which do not greatly affect its use in spectroscopic studies but do produce significant losses which affect the accurate determination of laser parameters.

Rh^{2+} ions have a $4d^7$ electronic configuration. Previous spectroscopic investigations[8] have demonstrated the existance of strong charge transfer absorption bands in the near u.v. spectral region between 300 and 400 nm. The fluorescence emission can occur either from the Stokes shifted charge transfer transition

or from d-d transitions after intersystem crossing. The relative importance of these two types of emission depends on the specific environment of the Rh^{2+} ion in the host crystal.[8] In $RbCaF_3$ crystals the Rh^{2+} emission comes entirely from spin allowed d-d transitions.

Figures 1 and 2 show the fluorescence emission spectra and lifetimes obtained at room temperature after excitation by the frequency tripled output of a mode-locked $Y_2Al_5O_{12}$:Nd laser. The excitation was at 354.7 nm with a 30 ps pulse. Similar results were obtained using a nitrogen laser which provides a 10 ns pulse at 337.1 nm. A 1/4-m monochromator with a PAR silicon diode array detector and optical multichannel analyzer were used to monitor the emission spectra, while the lifetimes were detected with an RCA C31034 phototube and photographed on a storage oscilliscope. For low energy excitation, the fluorescence spectrum appears as a broad band peaked at 710.0 nm with a full width at half maximum of about 16 nm and a fluorescence decay time of 9.0 μs. At high energy excitation, the position of the emission band remains unchanged but the halfwidth narrows to about 7 nm and the lifetime shortens to about 0.13 μs.

The abrupt lifetime shortening and spectral narrowing at a specific threshold pump energy are indicative of the onset of stimulated emission. In order to directly measure the effects of this "laser action", single pass gain measurements were performed using the experimental setup illustrated in Fig. 3. The tripled output from the $Y_2Al_5O_{12}$:Nd laser operating above threshold was used as the pump source and the output from a nitrogen laser-

pumped tunable dye laser was used as a probe beam. The dye used was a mixture of rhodamine 610 and oxazine 725 since this provided the ability to tune across the entire fluorescence emission band. A storage scope was used to measure the change in the probe beam intensity when the pump beam was turned on. Gain was observed in the tuning range from approximately 700 to 720 nm as shown in Fig. 1.

The results described above give the fundamental laser properties of $RbCaF_3:Rh^{2+}$ summarized in Table I. The peak gain coefficient was measured to be $\gamma=0.54\ cm^{-1}$. This can be used to determine the population inversion at threshold from the expression

$$\Delta N=8\pi\Delta\nu\tau\gamma n^2/\lambda^2. \qquad (1)$$

Here $\Delta\nu$, τ, and λ are the half-width, radiative lifetime, and peak position of the fluorescence band, respectively. Using the measured values for these parameters yields $\Delta N=3.4\times10^{17}\ cm^{-3}$. This number can be independently verified from the measured value of the pulsed pumping threshold energy density, $E_{th}=0.063\ J/cm^3$, which is related to the threshold population inversion by

$$\Delta N=E_{th}/h\nu. \qquad (2)$$

From this approach, a value of $\Delta N=2.3\times10^{17}\ cm^{-3}$ is determined which is consistent with the value obtained from gain measurements. For simplification, an intermediate value of $\Delta N=3\times10^{17}$ is listed in Table I and used to calculate the peak stimulated emission cross section from the relationship

$$\sigma_p=\gamma/\Delta N. \qquad (3)$$

This is also given in the table. The value of the cross section obtained from these measurements is consistent with the value

predicted from spectral parameters using the equation

$$\sigma_e = \lambda_p^2 / [8\pi c n^2 \Delta\tilde{\nu} \tau_f]. \quad (4)$$

The exact values of the laser parameters listed in Table I must be considered as only rough estimates due to several factors. These include perturbations associated with scattering losses because of poor sample quality, feedback due to cleaved sample faces, and unknown properties such as the exact value of the quantum efficiency. Despite these uncertainties, the measured values of gain and cross section are very favorable compared to those of other vibronic laser systems based on 3d transition metal ions. The symmetric shape of the emission band and tuning curve indicates that excited state absorption does not effect the stimulated emission properties of this material.

The results reported here are unique in two aspects: This is the first observation of stimulated emission and tunable gain in a crystal with a 4d transition metal as the active ion, and the first solid state laser system pumped through a charge transfer band. This suggests that many different 4d and 5d transition metal ions as well as other charge transfer molecular ions in solids may be useful in tunable solid state laser systems.[8] The future potential of these materials depends on the development of improved crystal quality which should reduce scattering losses and increase the fluorescence lifetime. When such samples are obtained, an attempt will be made to flashlamp pump the system.

ACKNOWLEDGMENTS. This work was sponsored by the U.S. Army Research Office and by the Office of Naval Research.

TABLE I. Spectral and Laser Parameters for $RbCaF_3:Rh^{2+}$ Crystals

Spectral Parameters	Laser Parameters
λ_p (nm)=710	E_{th} (J/cm^3)=0.063
$\Delta\lambda_{1/2}$ (nm)=17	ΔN_{th} (cm^{-3})=3x10^{17}
τ_f (μs)=9.0	γ (cm^{-1})=0.54
σ_e (cm^2)=1.1x10^{-18}	σ_p (cm^2)=1.8x10^{-18}
	Tuning Range: 700-720 nm

REFERENCES

1. P.F. Moulton, "Tunable Paramagnetic Ion Lasers", in Laser Handbook, Vol. 4, M. Bass and M. Stitch, eds. (North Holland, Amsterdam, in press).
2. L.F. Johnson, R.E. Dietz, and H.J. Guggenheim, Phys. Rev. Lett. 11, 318 (1963) and Appl. Phys. Lett. 5, 21 (1964); L.F. Johnson, H.J. Guggenheim, and R.A. Thomas, Phys. Rev. 149, 179 (1966); F. Johnson, H.J. Guggenheim, D. Bahnck, and A.M. Johnson, Opt. Lett. 8, 371 (1983); L.F. Johnson and H.J. Guggenheim, J. Appl. Phys. 38, 4837 (1967); B.C. Johnson, R.F. Moulton, and A. Mooradian, Opt. Lett. 10, 116 (1984); and P.F. Moulton, A. Mooradian, and T.B. Reed, Opt. Lett. 3, 164 (1978).
3. M.L. Shand and J.C. Walling, IEEE J. Quantum Electron. QE-18, 1829 (1982); J. Walling, O.G. Peterson, H.P. Jenssen, R.C. Morris, and E.W. O'Dell, IEEE J. Quantum Electron. QE-16, 1302 (1980).
4. S.T. Lai and M.L. Shand, J. Appl. Phys. 54, 5642 (1983).
5. U. Brauch and U. Durr, Opt. Lett. 9, 441 (1984) and Opt. Comm. 49, 61 (1984); U. Durr, U. Brauch, W. Knierim, and C. Schiller, in "Proc. First Tunable Solid State Laser Conference, La Jolla, June 1984" (Springer-Verlag, Berlin, in press).
6. J. Drube, B. Struve and G. Huber, Appl. Phys. B28, 235 (1982); ibid, B30, 117 (1983) and Opt. Comm. 50, 45 (1984).
7. P.F. Moulton, Opt. News 8, 9 (1982).
8. R.C. Powell, R.H. Schweitzer, J.J. Martin, G.E. Venikouas,

and C.A. Hunt, J. Chem. Phys. 81, 1178 (1984); R.C. Powell, J.J. Martin, R.H. Schweitzer, G.C. Gilliland, G.E. Venikouas, and C.A. Hunt, in "Proc. Conf. on Lasers and Applications, 1983", ed. R.C. Powell, (STS Press, Mclean, VA, in Press); and R.C. Powell in "Proc. First Tunable Solid State Laser Conference, La Jolla, June 1984" (Springer-Verlag, Berlin, in Press).

9. F.A. Modine, E. Sonder, W.P. Unruh, C.B. Finch, and R.D. Westbrook Phys. Rev. B 10, 1623 (1974).

FIGURE CAPTIONS

FIG. 1. Room temperature emission spectra and gain of a $RbCaF_3:Rh^{2+}$ crystal. The solid line is the fluorescence emission with peak pumping pulse energy density below threshold while the dashed broken curve is the fluorescence after pumping above threshold. The circles are the results of single pass gain measurements.

FIG. 2. Room temperature fluorescence decay time of $RbCaF_3:Rh^{2+}$ as a function of peak pumping pulse energy at 354.7 nm.

FIG. 3. Block diagram of experimental setup for single pass gain measurements.

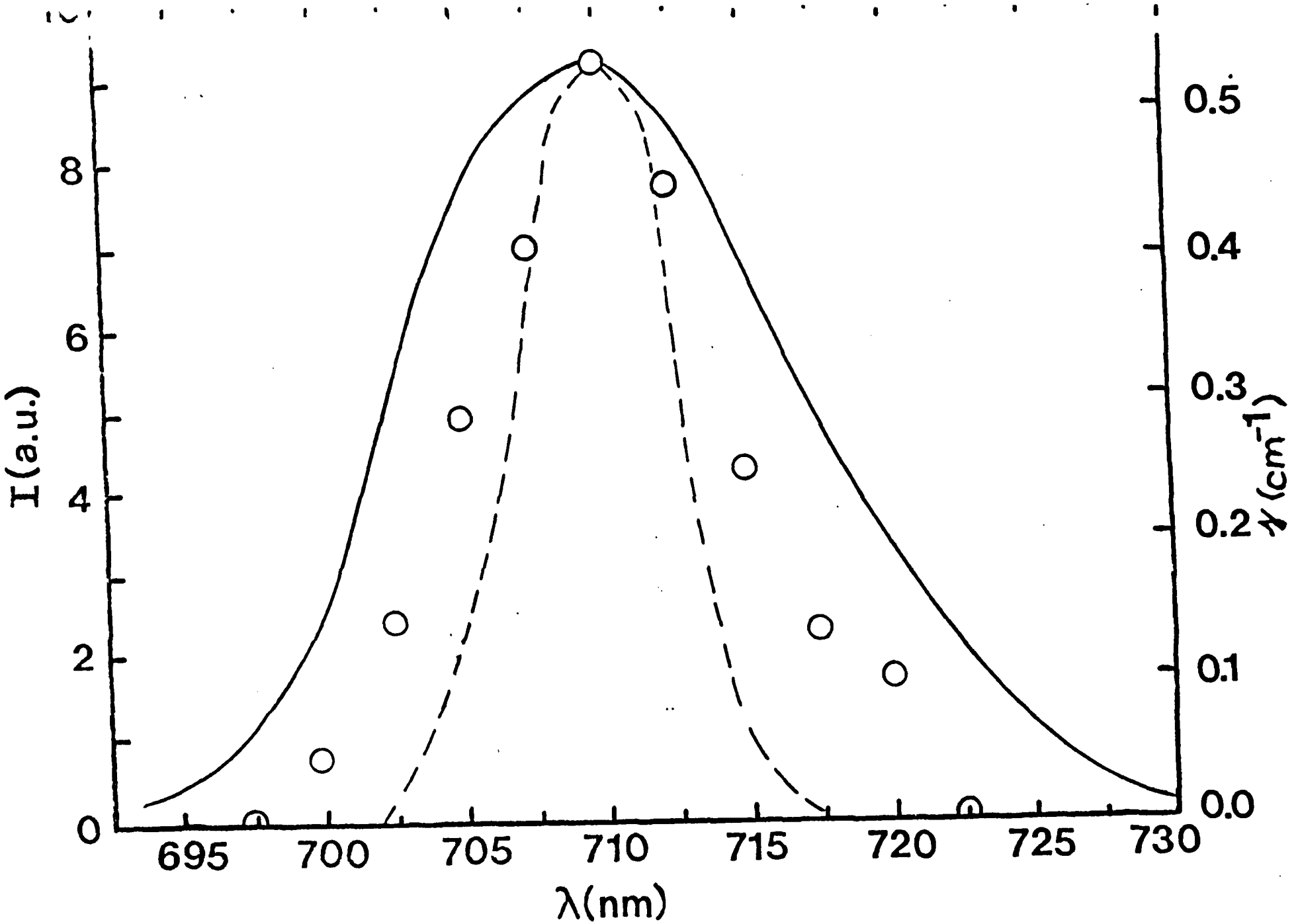
I(a.u.)
0
2
4
6
8
0.0
0.1
0.2
0.3
0.4
0.5
γ (cm⁻¹)
695
700
705
710
715
720
725
730
λ(nm)

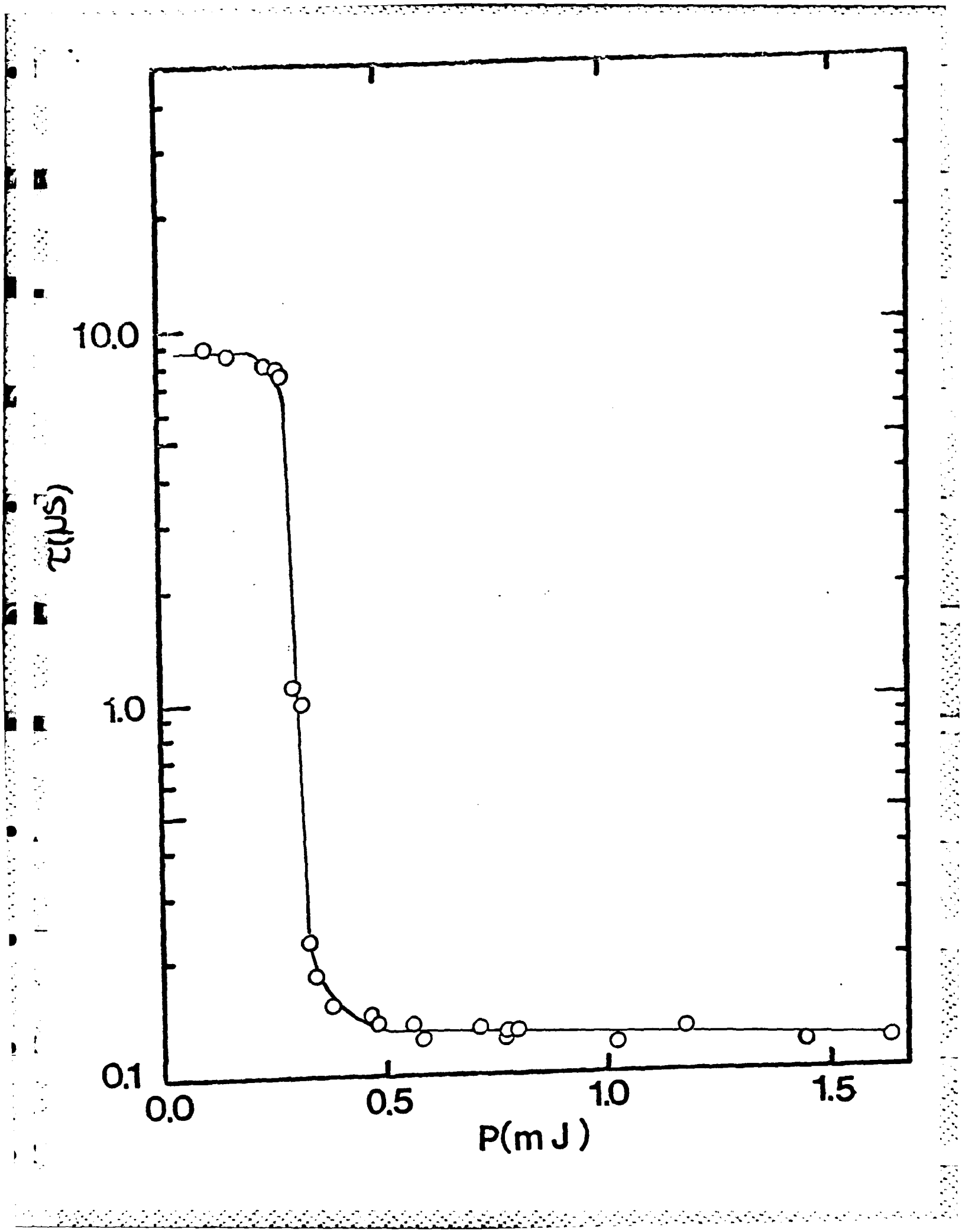
10.0
1.0
0.1
τ(μs)
0.0
0.5
1.0
1.5
P(mJ)

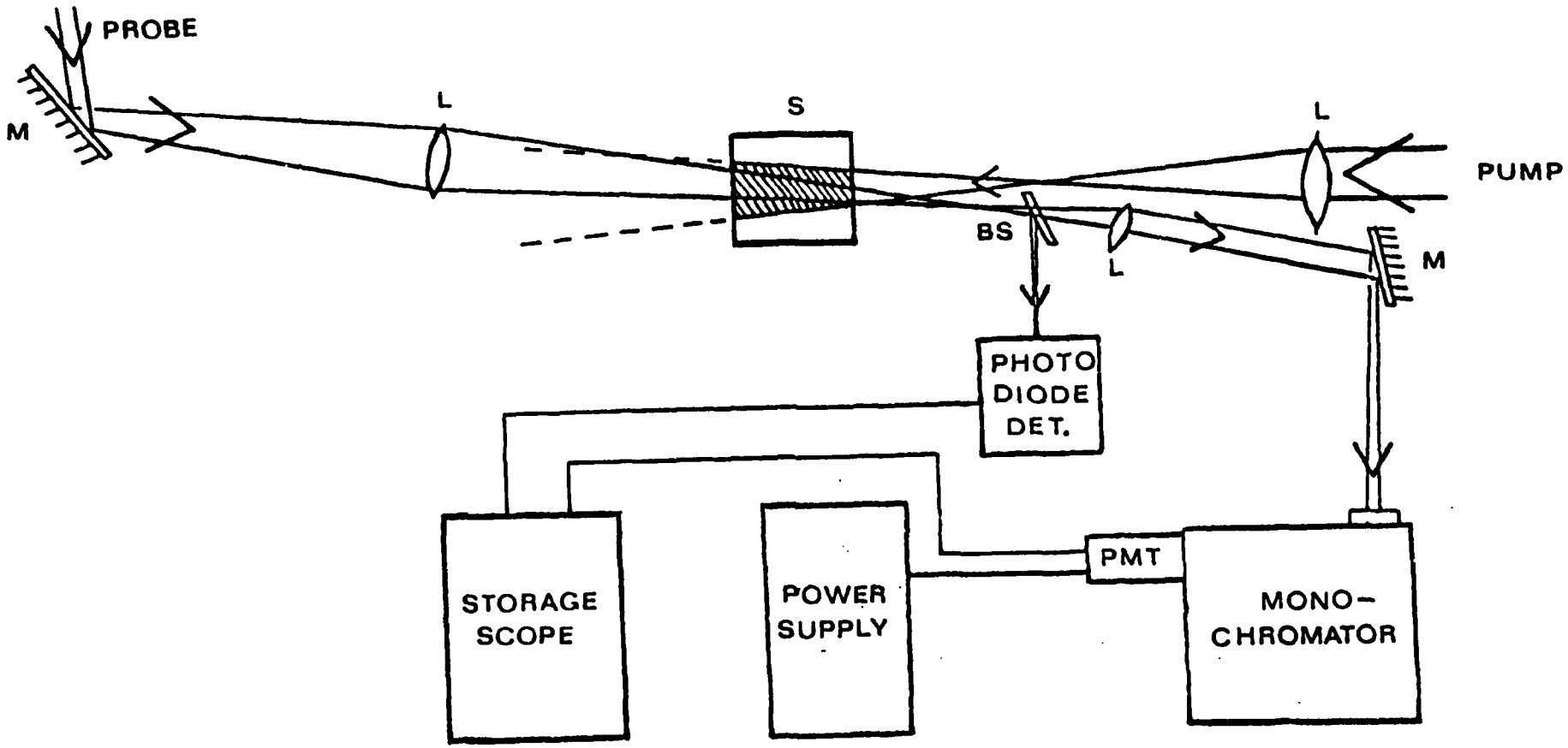
PROBE
M
L
S
L
PUMP
BS
L
M
PHOTO
DIODE
DET.
STORAGE
SCOPE
POWER
SUPPLY
PMT
MONO-
CHROMATOR

III. SPECTROSCOPIC PROPERTIES OF OTHER TRANSITION METAL ION-DOPED CRYSTALS

The following three sections describe the results of a survey of the optical properties of several potential laser materials. The Na β"-alumina material is an attractive host because of its high ionic conductivity. This means doping ions can be diffused into the hosts after growing undoped crystals. Although this has proven to be successful for Nd^{3+} laser crystals, our attempts to dope this material with transition metal ions resulted in poor optical quality samples. Most of the other host crystals investigated had problems with quality. The $Bi_4Ge_3O_{12}$ crystals exhibited sever laser damage problems. The only material which appears to have a high potential for possible tunable laser applications is Mn_2SiO_4. The optical properties of this material are summarized in Sec. III.3. The samples available during this investigation contained a significant amount of defects which made them unsuitable for laser studies. We are currently attempting to obtain crystals of higher optical quality to continue research and development on this material.

III.1 Na β"-Alumina as a Host Crystal

Beta aluminas are well known as solid electrolytes because of their high ionic conductivity (e.g., J.B. Bates, et al., Physics Today 35,46 (1982)). Recently it has been shown that this type of material can be used as a host for various luminescent impurity ions (B. Dunn and G.C. Farrington, Solid State Ionics 9&10, 223 (1983)) and laser action has been obtained in a Nd^{3+} doped sample (M. Jansen, et al., Opt. Lett. 9, 119 (1984)). The main interest in this type of material for a laser host crystal is due to the ability to diffuse high concentrations of doping ions into the open planes of the crystal and have very weak ion-ion interaction. We attempted to produce crystals of this material doped with Cr^{3+} or with Rh^{2+} for possible tunable laser applications. The spectroscopic properties of these samples are described in this section.

Several single crystals of $Na_{1.67}Mg_{0.67}Al_{10.33}O_{17}$ were obtained from Dr. J.B. Bates of Oak Ridge National Laboratory. These were in the form of platelets a few millimeters square and about a millimeter thick. They had excellent optical quality. Two methods were attempted to diffuse ions into these crystals. In the first method, the undoped crystal was placed in a crucible and surrounded by a powder containing the desired doping ions. The crucible was then heated to 700 C for several hours. The second method was similar except the crystal was suspended on a wire above the melt instead of being immersed in it. In both cases the crystals colored deeply indicating a high percentage of ion exchange. The Cr^{3+} doped samples turned green and the Rh^{2+} samples red.

The absorption spectra for Rh^{2+} and Cr^{3+} ions in Na β"-alumina crystals are shown in Fig. 1. The Rh^{2+} absorption is again a charge transfer band in the near u.v. spectral region while the Cr^{3+} doped crystal exhibits a broad structured absorption band peaking around 670 nm.

The fluorescence spectra at two times after the nitrogen laser excitation pulse at both 300 K and 10 K are shown in Figs. 2 and 3. The spectra of both samples consists of broad, double peaked emission bands. For Cr^{3+} the maxima occur at about 700 and 820 nm while for Rh^{2+} the maxima are at about 600 and 700 nm. The spectral dynamics of both systems can be explained in terms of the configuration coordinate diagram model shown in Fig. 10 of Sec. II.1.

The fluorescence lifetime of the 820 nm band of the Cr^{3+} doped sample is about 54 μs and independent of temperature whereas the lifetime of the 700 nm band decreases from 2.3 ms at 10 K to about 1.2 ms at 300 K.

The sharper band near 700 nm is probably due to emission from the ^2E level of Cr^{3+} (R-lines) broadened significantly by the random distribution of different types of crystal field sites in this type of crystal. The broad 820 nm band can be attributed to Stokes shifted emission from the $^4T_2$ level. The variation of the relative intensities of these bands with temperature and with time after the laser pulse and the temperature dependence of the fluorescence lifetimes can all be attributed to the rearrangement of the occupancy of these levels in thermal equilibrium.

A similar analysis can be used to explain the spectral

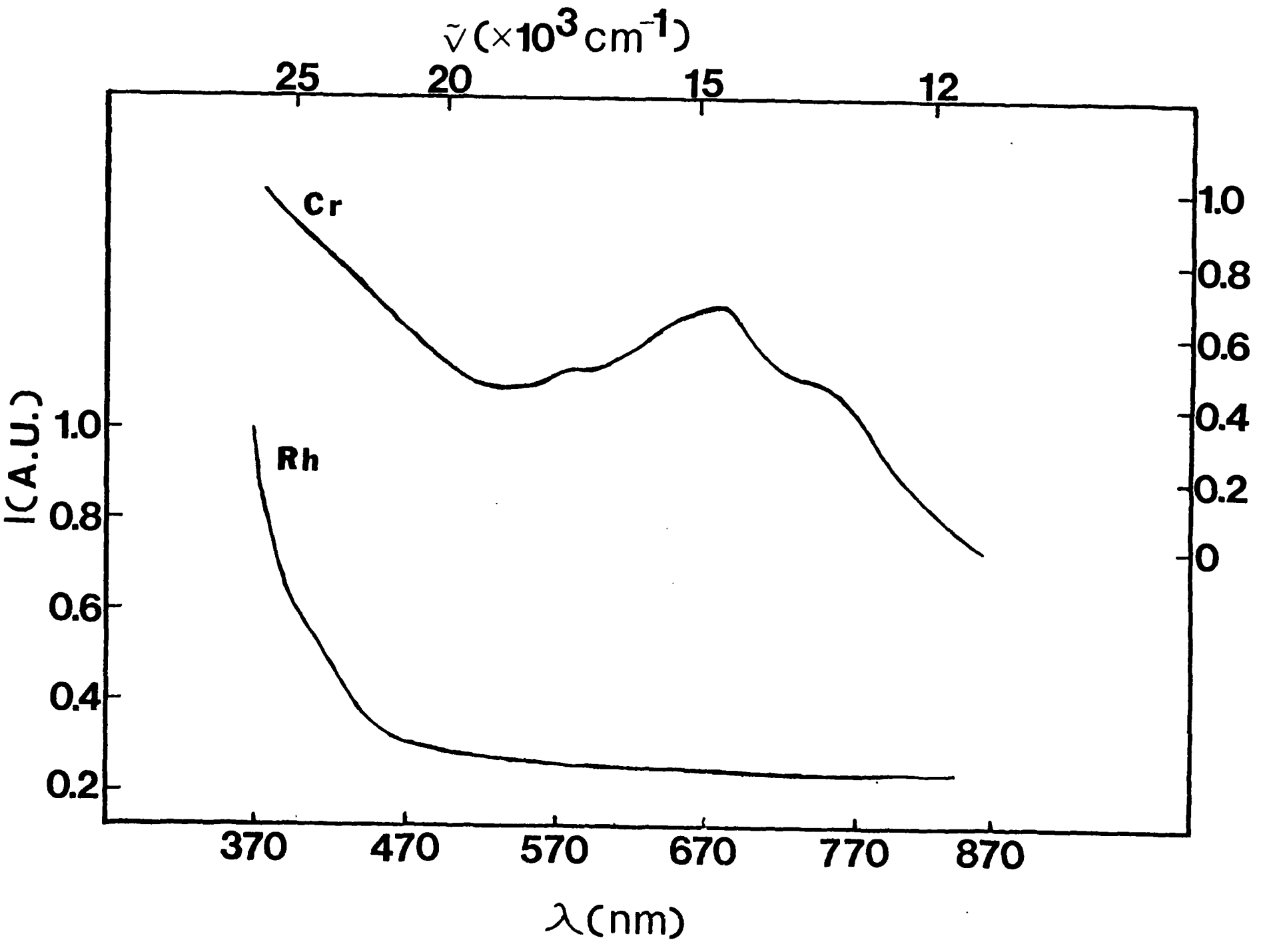

Fig. 1 Room temperature absorption spectra of Cr^{3+} and Rh^{2+} ions

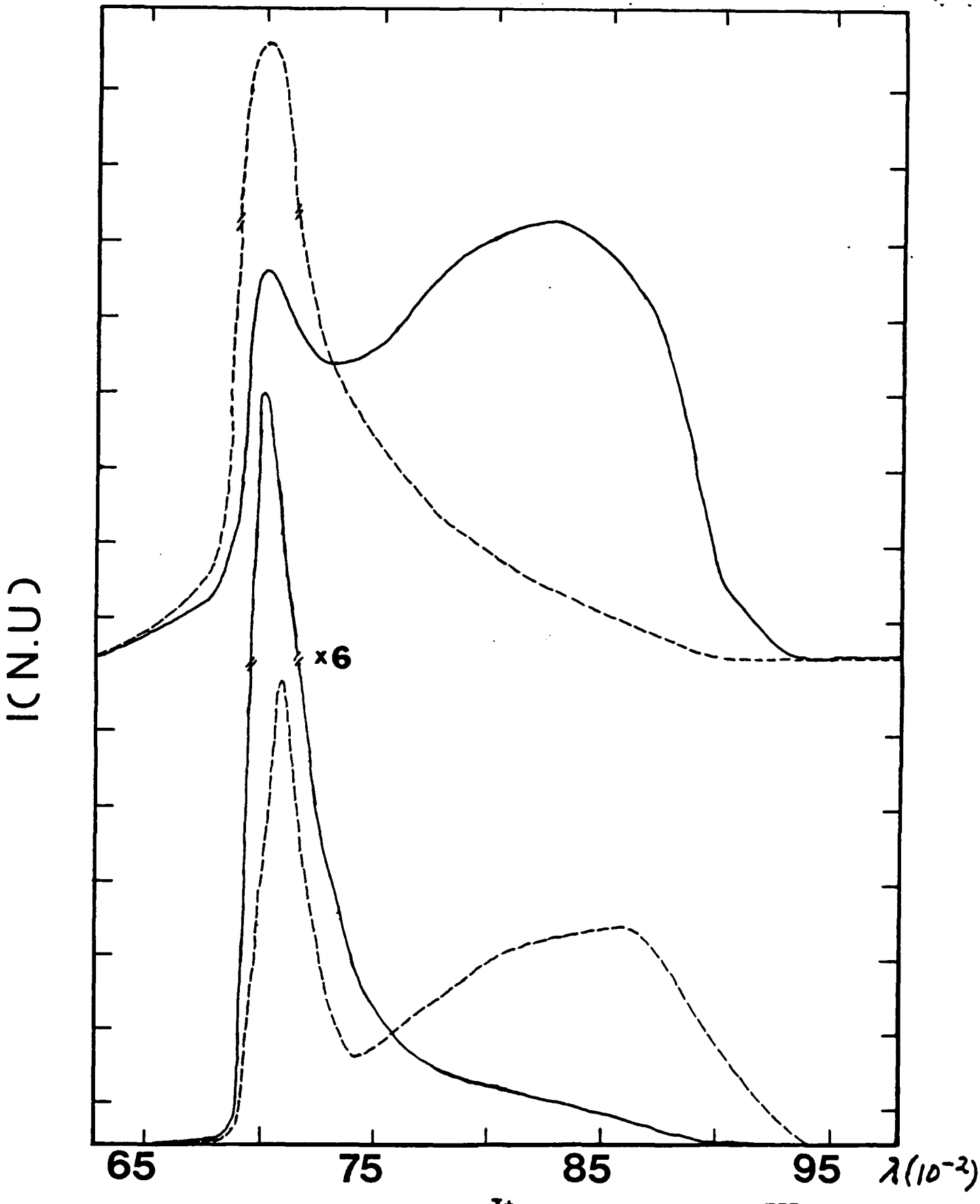

Fig. 2 Fluorescence spectra of Cr^{3+} in Na β"-alumina. TOP: T=300 K; solid line for 25 μs after excitation pulse; broken line for 200 μs after excitation pulse. BOTTOM: T=10 K; broken line for 25 μs after the excitation pulse; solid line for 200 μs after the excitation pulse.

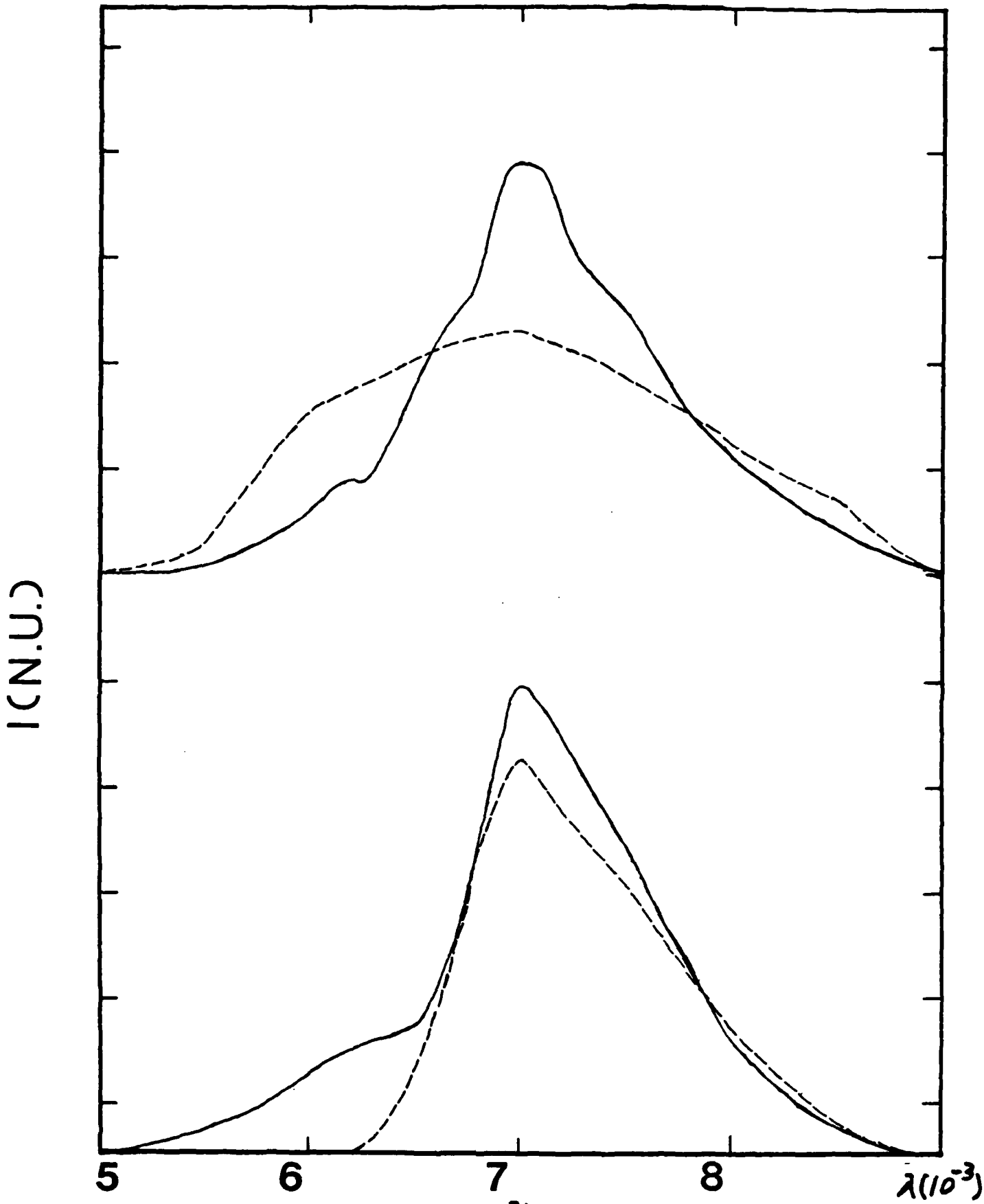

Fig. 3 Fluorescence spectra of Rh^{2+} in Na β"-alumina. TOP: T=10 K; solid line for 25 βs after excitation pulse; broken line for 200 βs after excitation pulse. BOTTOM: T=300 K; broken line for 25 μs after excitation pulse; solid line for

properties of the Rh^{2+} doped sample. The 700 nm emission band has fluorescence decay time of about 8 ms independent of temperature which is consistent with a spin-forbidden d-d transition. The lifetime of the 600 nm band decreases from 192 to 48 μs between 10 and 300 K. This is consistent with a spin-allowed d-d transition. The observed temperature and time dependences of the relative spectral emission intensities can be attributed to redistributing the excited state population between these two levels.

The fluorescence efficiencies, lifetimes, and bandwidths of both Cr^{3+} and Rh^{2+} doped Na β"-alumina crystals indicate they might be useful as tunable, solid state platlet lasers. The major problem in developing these materials for lasers is sample quality. For both dopants, the ion exchange process greatly degraded the optical quality of the original crystals. We believe the problem involves size mismatches of the doping ions in the lattice. This produces internal stress which causes the surface layers to flake off the sample. Solving this problem will require a significant amount of materials science development on this type of crystal.

III.2

SPECTROSCOPIC SURVEY OF SOME NEW TRANSITION METAL ION-HOST STRUCTURES

S. Colak, G.M. Loiacono, G. Mizell, W.K. Zwicker
Philips Laboratories, 345 Scarborough Rd., Briarcliff Manor, NY 10510

R.C. Powell
Oklahoma State University, Stillwater, Oklahoma 74074

Abstract

A number of luminescent ion-host crystal combinations were grown and preliminary spectroscopic studies on these crystals were done. This survey involves most of 3d transition metal ions, and some other ions of different series in various crystal sites. The host crystals are $Bi_4Ge_3O_{12}$, $KTiOPO_4$, $Cs_2NaBiCl_6$, Mn_2SiO_4, and $V(PO_3)_3$. The results of this preliminary survey are given in the form of transmission and luminescence spectra, and electronic level assignments.

Introduction

During the recent years there has been increasing interest in finding and studying new solid state laser hosts for laser ions, especially transition metal (TM) ions. Due to the lack of a unified predictive model for TM ion behavior in different hosts, the information on these ions still has to be collected from experiments. The purpose of the present work is to broaden our experimental knowledge on TM ion-host combinations in order to ease the future predictions in this field. In the following paragraphs, we will describe the growth of, and preliminary spectroscopic work on some new ion-host structures, and try to identify their behavior by comparing them to, and extrapolating from previously studied cases.

Experiments and Results

During this work we have tried to prepare a number of ion/host compounds such as all 3d ions and Pd, Os, Ce, Sm, Tb, in $Bi_3Ge_4O_{12}$ (BGO); Cr^{3+}, V^{3+}, Tb^{3+} in $KTiOPO_4$ (KTP); Ni, Ru, Pd, Os, in $Cs_2NaBiCl_6$ (CNBC); and studied fully concentrated Mn_2SiO_4 and $V(PO_3)_3$ crystals. The transmission spectra of the polished samples from these crystals were studied between 200 nm and 2500 nm, with some studies extending up to 10 μm. The luminescence was studied in the visible and in the near IR. The energy level assignments of the d-electron bands were done either by using published data, or with the help of Tanabe-Sugano diagrams[1-2] by using extrapolated rough values for the crystal field parameter, Dq, and interelectronic repulsion parameter B.

$Bi_3Ge_4O_{12}$ (BGO) crystals were grown by Czochralski method at around 1000°C under an oxygen atmosphere in a platinum crucible. BGO has been previously studied for its electro-optic properties[3], scintillation properties[4], its intrinsic luminescence[5] due to Bi, and also as a laser host for mainly rare earth ions[6] possibly with energy transfer[7]. The impurity ion content in the crystals grown here were less than 1%. Crystals grown with Ti, Pd, and Os had no indications of any absorption peaks within our range up to 2.5 μm. Cu, Fe and Ni doped samples showed very broad and weak absorption bands which were difficult to distinguish from the background. Clear gray colored Co:BGO had well defined absorption peaks in the visible, and some weak broad bands in near IR which were difficult to identify. The absorption bands of V, and Cr in BGO were well defined, but no luminescence was observed although various pump wavelengths at different temperatures were tried. The transmission spectra of vanadium in BGO given in Figure 1 can be fit best to V^{4+} in tetrahedral Ge site with Dq = 1000 cm^{-1} as extrapolated from Dq = 900 of VCL_4[8]. The band between 300-500 nm is assigned to charge transfer (CT) transitions due to its strength. Previous studies on vanadium in tetrahedral sites of GaAs[9], and II-VI[10-12] compounds show that this ion is either in V^{2+} or V^{3+} form with varying Dq and B parameters. In our case, extrapolated Dq and B values for V^{2+} and V^{3+} require additional absorption bands which we could not detect. An approximate fit to the spectra of chromium doped BGO given in Figure 2 can be found by assuming Cr^{3+}, Dq = 800 cm^{-1}, and B = 500 cm^{-1}. No luminescence was detected from this material either. We have not observed any indication of photochromic effects as reported for $Bi_{12}GeO_{20}:Cr^{2+}$, Cr^{3+} [13]. BGO with manganese is the only sample in this group which luminesced. The transmission spectra given in Figure 3 can be identified with Mn^{4+}, Dq = 1400 cm^{-1}, B = 700 cm^{-1}. The emission spectra is shown in Figure 3 and the nonexpotential decay time is between 3.5 and 9 μsec. The possibility that the emission is due to Bi excited by double photon absorption is

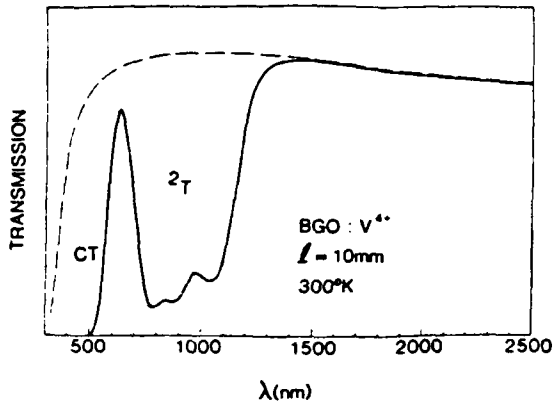

Figure 1. Transmission spectra of 0.5% vanadium in $Bi_4Ge_3O_{12}$. Dashed curve indicate host transmission.

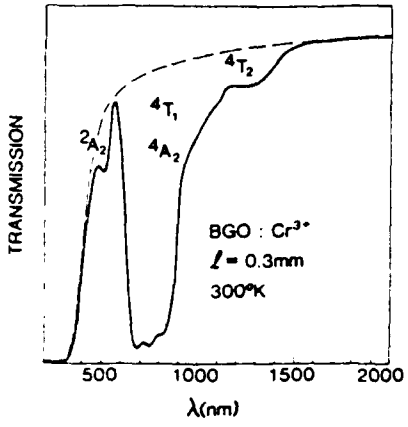

Figure 2. Transmission spectra of 0.5% chromium in BGO.

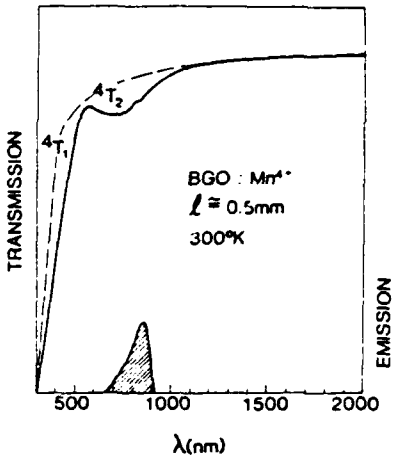

Figure 3. Transmission and emission spectra of 0.5% manganese in BGO. Shaded band indicate emission with decay time between 3 μsec and 9 μsec.

excluded because Bi decay is faster[5,7] than values given above. Ce in BGO gave a charge transfer band between 300 nm and 450 nm, and another narrow band around 3 μm which can be assigned to $^4F_{7/2}$ states of Ce^{3+}. Tb in BGO gave typical Tb^{3+} spectra with a strong $^5D_4$ --> $^7F_5$ branching ratio and lifetime of $^5D_4$ was about 1.5 msec. Similarly Sm in BGO showed typical Sm^{3+} peaks, with emission most probably originating from $^4G_{5/2}$ states.

The growth techniques of the $KTiOPO_4$ (KTP) crystals will be reported elsewhere. This material has previously been studied[14] for its nonlinear optical properties. Cr, V, and Tb were incorporated in this material at levels less than 1%. The transmission, and emission spectra of KTP:Cr^{3+} sample is shown in Figure 4. Peak absorption cross section of at 650 nm is estimated to be in the 10^{-19} cm^2 range. This high value may be due to the distored octahedral lattice site of the host. The absorption spectra can be fit by using Dq = 1600 cm^{-1} and B = 800 which is very similar to the situation in other hosts. The lifetime of $^4T_2$ emission is 5 μsec at 300°K, and 95 μsec at 10°K with similar band shapes at both temperatures. The transmission spectra of vanadium doped KTP samples below 1 μm was very similar to Cr doped samples, and it could be identified with V^{3+}, Dq = 1700 cm^{-1}, and B = 850 cm^{-1}. The absorption bands of KTP:V^{3+} also fits to the spectra given for Al_2O_3:V^{3+} [15] except that we could not detect any $^1T_2$, ^1E lines around 10^4 cm^{-1}. Although we have observed near IR luminescence from KTP:V^{3+} samples, additional experiments are necessary to determine that this emission is not related to Cr^{3+} impurities which has similar emission spectrum and decay times. Only weak luminescence from V^{3+} has been observed previously in Al_2O_3:V^{3+} [16-17] with both narrow line and broad band forms at various energies[17]. Tb doped KTP showed typical Tb^{3+} spectra with $^5D_4$ decay times in the order of 10^{-3} seconds.

A set of elpasolite crystals with $Cs_2NaBiCl_6$ (CNBC) composition[18-19] were grown by the Bridgeman method. This crystal has an absorption edge at about 400 nm, and is water soluble. The incorporation of Ni, Ru, Pd, and Os ions in the crystal were done at about

1 w/o level. Incorporation of Ni produced pink transparent crystals with weak and broad absorption bands in the visible and in near IR. Ru doping resulted in black crystals because of a featureless strong absorption band between 400 and 650 nm which is most probably due to charge transfer transitions. Pd doping resulted in yellowish crystals with a small shoulder near the intrinsic absorption edge of the material. No other bands in this material could be detected in the visible and near IR region. The Os doped samples showed distinct absorption bands as seen in Figure 5. This spectra can be fit best to the extrapolated form of Tanabe-Sugano diagram for d^2 with B = 300 cm^{-1}. This suggests Os^{6+} in octahedral site with Cl neighbors. Although the possibilities of Os^{4+} and Os^{5+} can not be excluded totally, the fits for them are not as good. The preliminary experiments did not show any visible or near IR luminescence from any of these samples.

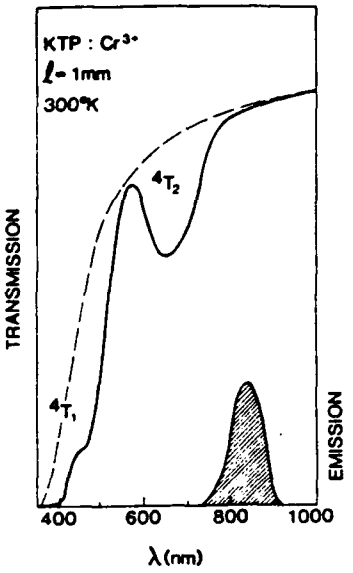

Figure 4. Transmission and emission spectra of about 0.1% Cr^{3+} in $KTiOPO_4$. The lifetime of emission is about 5 μsec.

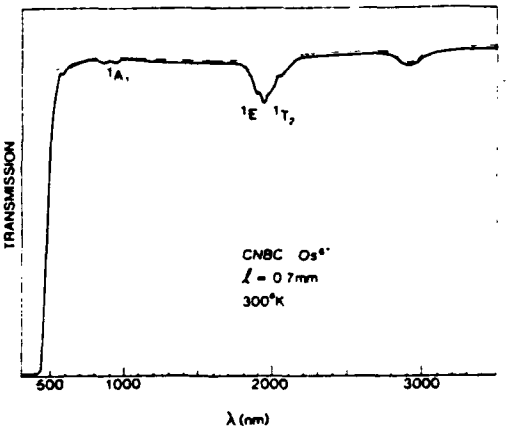

Figure 5. Transmission spectra of Osmium (≤ 1%) in $Cs_2NaBiCl_6$.

Absorption band for Mn_2SiO_4 shown in Figure 6 fits Mn^{2+} in octahedral site with Dq = 870 cm^{-1} and B = 720 cm^{-1}. As shown in Figure 6 the material luminesces around 700 nm with a decay time of about 3.6 μsec at 300°K. The 77°K emission spectra is similar to 300°K spectra, and the luminescence decay at 77°K is a double exponential with 0.76 and 1.3 msec decay times. The Mn^{2+} ion in Zn_2SiO_4 is a well known green phosphor[20] with emission decay times in the order of 10^{-2} seconds[21]. Slightly different crystal structures in Mn_2SiO_4 is the cause of the emission shift, and the lifetime decrease is expected due to high Mn^{2+} concentration. In fact at fully concentrated materials, one would expect total quenching of luminescence at room temperature due to efficient collective excitation transfer[22] among ions toward traps. This rapid energy transfer might also be used[22] to energy transfer similar to the case in Cr^{3+}, Nd^{3+} doped garnets[23]. Mn_2SiO_4 has been studied previously for its materials properties[24-25].

The samples of $V(PO_3)_3$ showed V^{3+} absorption structure which fit to Tanabe-Sugano diagrams with Dq = 1600 cm^{-1} and B = 800 cm^{-1} in octahedral site symmetry as seen in Figure 7. The luminescence was detected only at 10°K from (^1E,$^1T_2$) and ($^1A_1$) to ground $^3T_1$ states with approximately 10 nsec decay time. The splitting in the emission lines may be due to either collective behavior[22] of highly concentrated V^{3+} ions, or ground state splittings as was observed with a different structure for V^{3+}:Al_2O_3 case[17].

Conclusions

Our survey study on the incorporation of 3d ions, and Pd and Os in $Bi_4Ge_3O_{12}$ did not result in any promising luminescence from these materials. Only in the case of Mn some weak luminescence peaking around 850 nm could be found. These findings support the results of an independent study on a similar germanate host[26] doped by a variety of d-electron ions. The present, and earlier studies indicate that transition metal ions (especially 3d series) prefer the tetrahedral Ge site in this host.

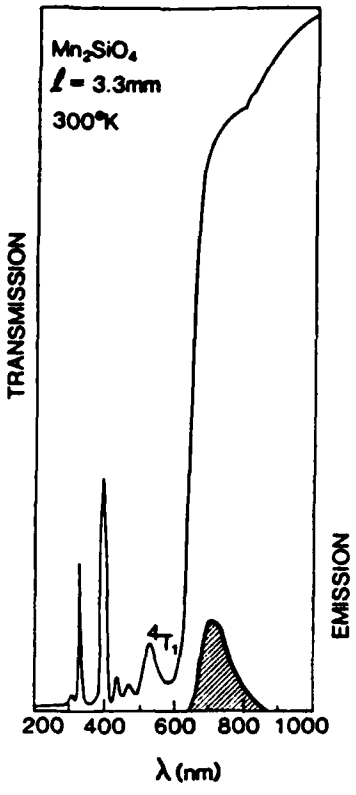

Figure 6. Transmission and emission spectra of Mn_2SiO_4 due to Mn^{2+}. Shaded band indicate emission.

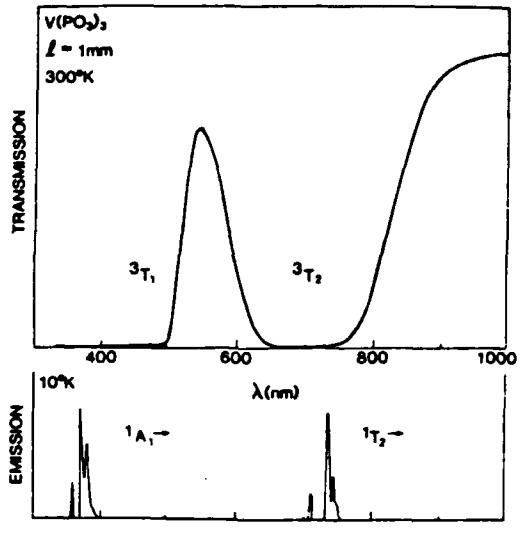

Figure 7. Transmission and emission (10°K) spectra of $V(PO_3)_3$.

$KTiOPO_4$ seems to accept 3d ions (Cr^{3+}, V^{3+}) readily in the distorted octahedral Ti site. Cr^{3+} showed luminescence with about 5 μsec decay around 840 nm. V^{3+} containing samples showed similar luminescence, but the origin of this luminescence is yet unknown.

The preliminary studies on Ni, Ru, Pd, and Os doped $Cs_2NaBiCl_6$ crystals did not show any luminescence at room temperature. Except for Os, the other three ions in this host resulted in broad and/or weak absorption bands which were difficult to identify.

Mn_2SiO_4 seemed to be the most promising candidate for further studies due to the strong luminescence of Mn^{2+} around 700 nm, with 3.6 μsec lifetime even at this fully concentrated limit. Crowded absorption band structure of Mn^{2+}, however, may cause an excited state absorption problem at high excitation conditions. This material may also be useful to host rare earth ions for lasing where Mn^{2+} is used for efficient energy transfer.

$V(PO_3)_3$ showed V^{3+} absorption bands and some luminescence could be detected from the samples only at 10°K.

A crude extrapolation technique was developed and used to find possible ranges for unknown Dq and B parameters for some ions. This helped to identify some of the spectra in this work, and it is expected to be useful for other new ion-host structures.

Acknowledgements

We would like to thank J. Jacco, M. Jaso, and T. Kovats for growing some of the crystals, to E. Jones, B. Greenberg, M. Frommer and T. McGee for materials analysis.

Appendix

Extrapolations for Unknown Dq and B Parameters.

Knowledge about the energy level structure of a TM ion in a host gives some information about the possible radiative and nonradiative processes. The first order electronic

states and approximate energy levels of an ion can be identified from Tanabe-Sugano diagrams if Dq and B parameters are known. As generally accepted this approach neglects other secondary parameters of ligand field theory, and is less acceptable for 4d, and 5d ions, or for cases where a molecular orbital approach[27] is more appropriate due to less localized d-electron wave functions. However, it is believed here that even a very rough knowledge on the energy levels with an extrapolated set of Dq and B can be useful where no information is available. To make such extrapolations one can start from the approximate factorizations developed for a number of ions and ligands[28]. These are

$$Dq = fg/10$$
$$\beta = B/B_o = 1 - hk \qquad (1)$$

where, h, f, g, and k are empirical parameters[2,29], and B_o is the free ion interelectronic repulsion parameter[29]. These parameters vary in an organized fashion, as one scans the periodic table within transition metal ions, and within nearest ligand ions. These variations can be approximated mostly with linearized values for neighboring ions in the periodic table . A set of unknown $(Dq)_2$, $(B)_2$ parameters can be found from known neighboring $(Dq)_1$, $(B)_1$ parameters by using

$$(Dq)_2 = (Dq)_1 \ (1 + \Delta_D) \qquad (2a)$$

$$\beta_2 = \beta_1 - \eta\Delta_B[1 - \beta_1] \qquad (2b)$$

where $\beta_2 = (B)_2/(B_o)_2$ and $\beta_1 = (B)_1/(B_o)_1$. If $(B_o)_2$ cannot be found from published tables than its value also can be extrapolated by using

$$(B_o)_2 = (B_o)_1 \ (1 + \Delta_O) \qquad (2c)$$

Δ_D, Δ_B, and Δ_O are fractional variations as one scans the periodic table in defined directions and their values are tabulated in Table 1. In the table, q is TM ion charge; N is the quantum number n for the open d-shell; M is the quantum number n for the neighbor host atom open shell; and e, and E are the number of missing electrons in the open shells of the transition metal ion and the host ion, respectively. η is an empirical function which can be taken as unity if $B/B_o = \beta$ is close to unity, otherwise one can use

$$\frac{1}{\eta} = 1 + \frac{3(1-\beta_1)^3\ |\Delta_B|}{(\beta_1-0.1)(\beta_2-0.1)}$$

The $(Dq)_2$ and $(B)_2$ extrapolations can be repeated forward, or backward by iteration, and examples of the results obtainable with such computations for octahedral sites are shown in Table 2. Table 2 also contains the results obtained by using Eq. (1), and the published experimental values obtained from various sources.

TABLE 1*. Extrapolation Parameters for D_q and B.

		Δ_D	Δ_B	Δ_O
ion	$q_2-q_1 = 1$	$\frac{0.8}{1+2(q_1-2)}$	$\frac{1.7}{1+3(q_1-2)}$	0.1
	$N_2-N_1 = 1$	$\frac{0.4}{N_1-2}$	- 0.2	$-[0.1 + (5-N_1) \times (4-N_2) \times 0.15]$
	$e_1-e_2 = 1$	- 0.0	+ 0.2	0.05
host	$M_2-M_1 = 1$	- 0.1	$\frac{0.9}{(M_1-1)^2}$	0
	$E_1-E_2 = 1$	- 0.1	- 0.2	0

* See Appendix for parameter definitions.

TABLE 2. Examples of Extrapolated Dq and B from Eq. (2) (in 10^3 cm^{-1}).

Ion	Oct. Host	Eq. 1 (a) Dq	B	Experimental	Dq	B	Eq. 2 (b) Dq	B	Eq. 2 (c) Dq	B
Co^{2+}	0	0.93	0.85	(d)	0.93	0.90	-	-	1.06	0.90
Cr^{3+}	0	1.60	0.70	(e)	1.65	0.65	1.67	0.74	1.91	0.76
Mn^{4+}	F	2.10	0.64	(f)	2.20	0.60	1.91	0.76	2.18	0.72
Rh^{3+}	Cl	2.20	0.29	(g)	2.10	0.32	1.90	0.35	2.17	0.34
Re^{4+}	Cl	2.80	-	(f)	3.30	0.36	2.90	0.35	-	-
Os^{6+}	F	-	-	(f)	3.60	0.40	4.14	0.45	4.74	0.38

(a) h,k,f,g taken from Ref. 2.
(b) Start from Co^{2+} in 0 host.
(c) Start from Re^{4+} in Cl host.
(d) Refs. 2 and 29.
(e) Ref. 30.
(f) Ref. 8.
(g) Refs. 8 and 31.

References

1. Y. Tanabe, S. Sugano, J. Phys. Soc. (Japan), 9, 753, 766, (1954).
2. B.N. Figgis, Introduction to Ligand Fields, (Interscience, 1966).
3. R. Nitsche, J. Appl. Phys., 36, 2358 (1965).
4. K. Takagi, et al., J. Crystal Growth, 52, 584, (1981).
5. M.J. Weber, R.R. Monchamp, J. Appl. Phys., 44, 5495, (1973).
6. A.A. Kaminskii, et al., Phys. Stat. Sol.(a), 56, 725, (1979).
7. D.P. Neikirk, R.C. Powell, J. Luminesc., 20, 261, (1979).
8. C.J. Ballhausen, Introduction to Ligand Fields, (McGraw-Hill, 1962).
9. A. Mircea-Roussel, et al., Solid State Commun., 36, 171, (1980).
10. L.M. Hoang, J.M. Baranowski, Phys. Stat. Sol. (b), 84, 361, (1977).
11. H. Sharg-ta, J. Luminesc., 24/25, 281, (1981).
12. S.W. Biernacki, Phys. Stat. Sol. (b), 118, 525 (1983).
13. W. Wardzynski, et al., Opt. Commun., 30, 203 (1979).
14. F.C. Zumsteg, et al., J. Appl. Phys., 47, 4980 (1976).
15. D.S. McClure, J. Chem. Phys., 36, 2757, (1962).
16. L.A. Riseberg, in Radiationless Processes, ed. by B. DiBartolo, (Plenum Press, 1980).
17. Z. Goldschmidt, et al., Phys. Lett., 19, 17, (1965).
18. A.T. Anistratov, et al., Sov. Phys. Solid State, 21, 1232, (1979).
19. B.V. Beznosikov, S.V. Mosyul, Sov. Phys. Crystallogr., 23, 346, (1978).
20. D.T. Palumbo, J.J. Brown, Jr., J. Electrochem. Soc., 117, 1184 (1970).
21. D.J. Robbins, et al., Electrochem. Soc. Ext. Abs., 82-1, 838, (1982).
22. G.F. Imbusch, in Luminescence of Inorganic Solids, ed. by B. BiBartolo, (Plenum Press, 1978).
23. D. Pruss, et al., Appl. Phys., B28, 355 (1982).
24. K. Fujino, et al., Acta Crystallogr, B37, 513, (1981).
25. J.P. Moore, C.B. Finch, J. Am. Ceram. Soc., 65, C184, (1982).
26. G. Huber, private communications on unpublished results.
27. A.M. Stoneham, Theory of Defects in Solids, (Clarendon Press, 1975).
28. C.K. Jorgensen, Disc. Farad. Soc., 26, 110 (1958). (See also Refs. 2 and 29).
29. J.S. Griffith, The Theory of Transition Metal Ions, (Cambridge Univ. Press, 1961).
30. D.L. Wood, in Optical Properties of Solids, ed. by S. Nudelman, S.S. Mitra, (Plenum Press, 1969).
31. C.S.G. Phillips and R.J.P. Williams, Inorganic Chemistry, Vol. II, (Oxford Univ. Press, 1966).

SPECTROSCOPIC EVALUATION OF Mn_2SiO_4 AS A POSSIBLE TUNABLE LASER MATERIAL

Lin Xi, Robert H. Schweitzer, and Richard C. Powell
Physics Department, Oklahoma State University
Stillwater, OK 74078

and

G.M. Loiacono and G. Mizell
Philips Laboratories
Briarcliff Manor, NY 10510

Abstract

Mn_2SiO_4 is a concentrated manganese system exhibiting broadband fluorescence at room temperature. Time-resolved spectroscopy results were obtained as a function of temperature and are analyzed to determine the ion-ion interaction and radiationless quenching properties of this material.

Mn^{2+} ions in crystals are known to have broad fluorescence emission bands.[1-4] The transition producing this emission is between the $^4T_{1g}$ and $^6A_{1g}$ levels of the $3d^5$ electron configuration shown in Fig. 1. Since this involves a redistribution of electrons between the crystal field split d states, the transition energy is sensitive to crystal field modulation and thus appears as a broad vibronic band. In normal Mn^{2+} doped crystals, the oscillator strengths of the absorption transitions are so small that the system can not be efficiently optically pumped. One way to overcome this problem is increasing the concentration of manganese ions. However, concentrated manganese systems generally exhibit strong radiationless quenching which leads to the disappearance of fluorescence at room temperature.[1-4]

Figure 2 shows the room temperature fluorescence emission of some concentrated manganese crystals whose spectral properties have not been previously characterized. The appearance of relatively strong room temperature fluorescence indicates weaker radiationless quenching than is present in other stoichiometric manganese crystals. To evaluate the potential usefulness of these materials in optical applications it is important to characterize the complete spectral dynamics of the system. The results of our investigation of the properties of Mn_2SiO_4 crystals are summarized below. The laser-excited, time-resolved spectroscopy setup used for this work has been described previously.

The fluorescence emission of Mn_2SiO_4 after pulsed laser excitation evolves in time from a band peaked at 700 nm to a band peaked at 800 nm. The time evolution of the ratio of the fluorescence intensities of the two bands at 150 K is shown in Fig. 3.

The relative intensities of the two bands vary significantly with temperature. The fluorescence lifetime of the 700 nm band decreases from about 3.17 ms at 10 K to about 1.33 μs at room temperature. The 800 nm band has a lifetime of about 700 μs at 50 K and about 1.93 μs at room temperature. In addition the long wave length band exhibits a rise time in its emission pattern which decreases from about 107 μs at 50 K to about 1.21 μs at room temperature.

The time and temperature dependences of the spectral dynamics described above can be interpreted using the model shown in Fig. 4. This is based on the concept of having Mn^{2+} ions in two nonequivalent types of sites in the lattice. The first are ions in normal lattice sites. These form an exciton band and directly absorb the pump light. At low temperatures, lattice relaxation around the excited ions causes a self-trapping of the exciton and fluorescence is emitted as the 700 nm band. At higher temperatures the exciton can become thermally activated and hop through the lattice until it becomes trapped at a Mn^{2+} ion with perturbed energy levels due to a neighboring chemical or structural defect. Ions in this type of site are the orgin of the 800 nm fluorescence. Using the parameters shown in Fig. 4, rate equations can be written to describe the time dependences of the concentrations of mobile and trapped excitons. The solutions of these equations are proportional to the fluorescence intensities from ions in the two types of sites. These equations can be fitted to the observed experimental data with the energy transfer rate, thermal quenching rate, thermal activation energies, and fractional concentration of defect sites treated as adjustible parameters. In addition, the rise time data provides the information necessary to separate the total transfer rate into its individual components representing the exciton diffusion rate and the trapping rate.

The parameters obtained from the model and fitting approach discussed above are summarized in Table I. The important conclusions from this analysis are: (1) The thermal quenching temperature of Mn^{2+} ions in normal lattice sites in this material is above room temperature. (2) Fluorescence quenching occurs because of efficient energy migration to Mn^{2+} ions in trapping sites. In the samples of Mn_2SiO_4 presently available, the concentration of trapping sites is quite high. If future developments in materials preparation are successful in decreasing the amount of chemical and structural defects in the crystals, it should be possible to produce concentrated manganese materials with spectral properties favorable for use in tunable solid state laser applications.

References

(1) K. Gooen, B. DiBartolo, M. Alam, R.C. Powell, and A. Linz, Phys. Rev. 177, 615 (1969).

(2) E.V. Matyushkin, L.S. Kukushkin, and V.V. Eremenko, Phys. Status. Solidi 22, 65 (1967); V.V. Eremenko, E.V. Matyushkin, S.V. Petrov, Phys. Status Solidi 18, 683 (1966); and V.V. Eremenko and E.V. Matyushkin, Opt. i Spektroskopiya 23, 437 (1967) [English transl.: Opt. Spectry. (USSR) 23 234 (1967)].

(3) J. Danko, D. Bacheco, and B. DiBartolo, Phys. Rev. B 28, 2382 (1983).

(4) R.L. Green, D.D. Sell, and R.M. White, in "Optical Properties of Ions in Crystals", edited by H.M. Crosswhite and H.W. Moos (Interscience Publishers, New York, 1967), p. 289.

TABLE I. Summary of Results

τ_S^O=3.17 ms	τ_B=67 ns
τ_T^O=0.70 ms	τ_Q=21 ns
k_D^{-1}(150 K)=76 μs	k_T^{-1}=4.0 μs
ΔE_{SB}=612 cm^{-1}	ΔE_D=15 cm^{-1}
ΔE_Q=938 cm^{-1}	N_T/N_S=0.1

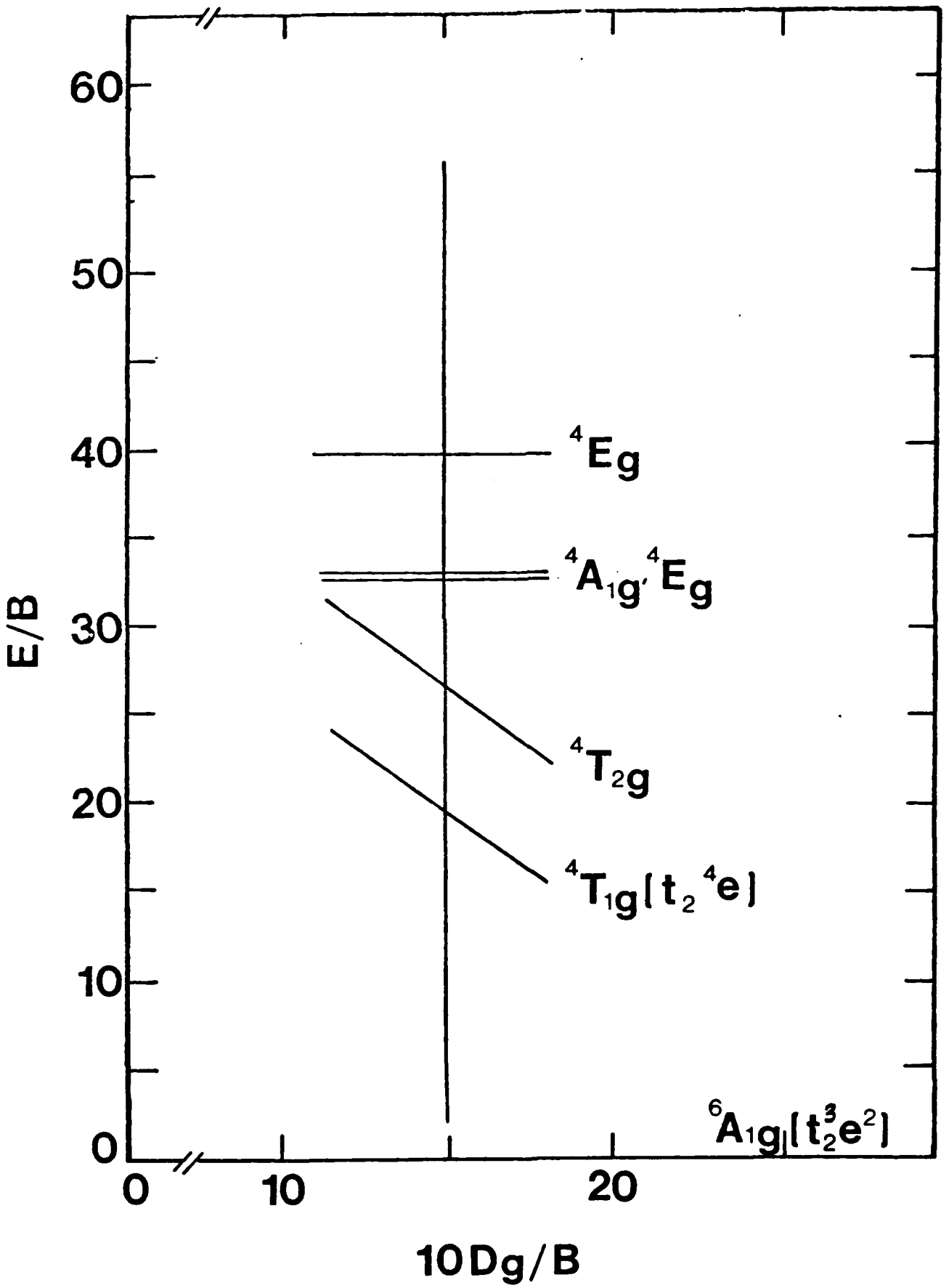
60
50
40
30
20
10
0
E/B
0
10
20
10Dg/B
^4Eg
$^4A_{1g}, ^4Eg$
$^4T_{2g}$
$^4T_{1g}[t_2{}^4e]$
$^6A_{1g}[t_2^3e^2]$

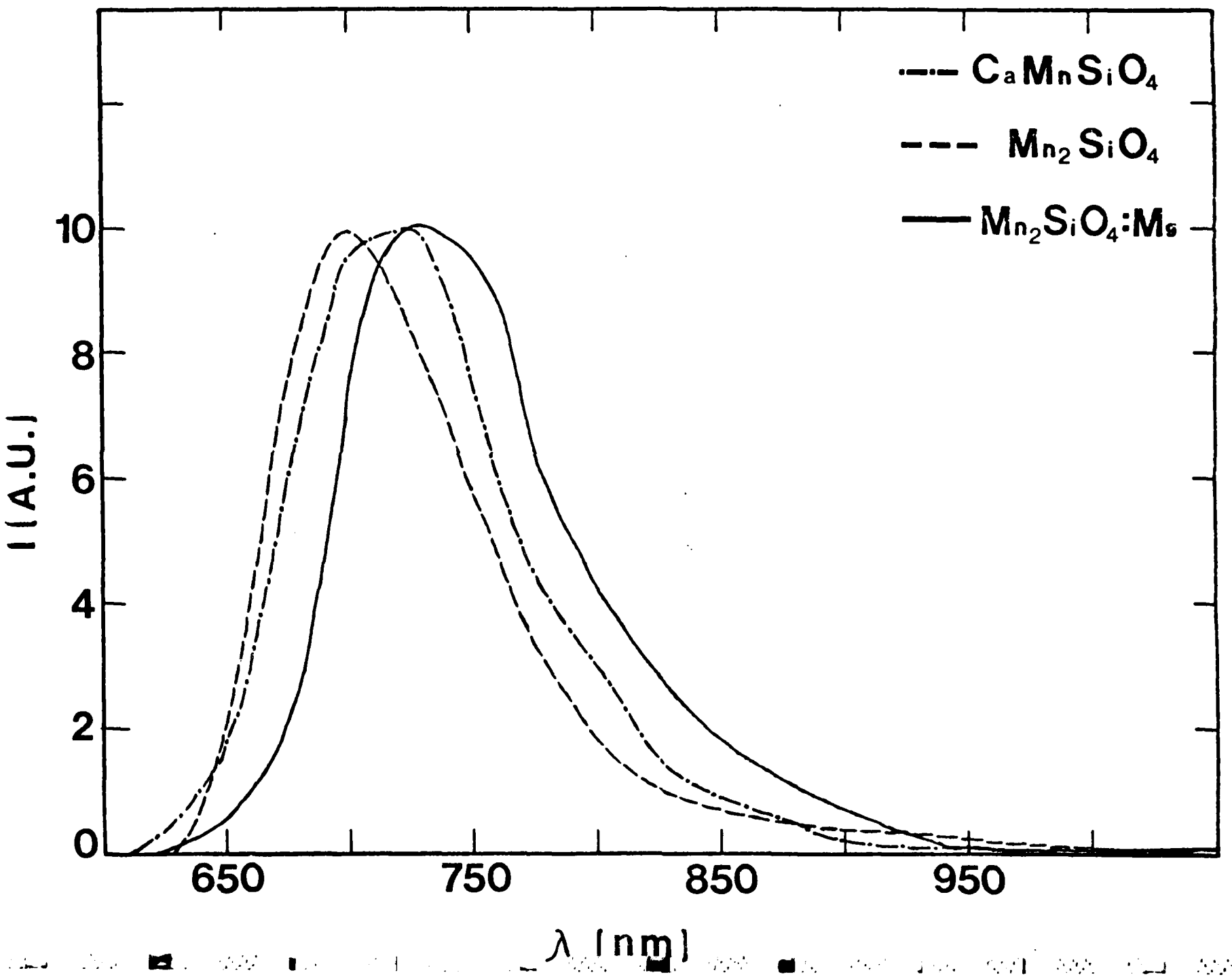
CaMnSiO4
Mn2SiO4
Mn2SiO4:Ms
I(A.U.)
0
2
4
6
8
10
650
750
850
950
λ [nm]

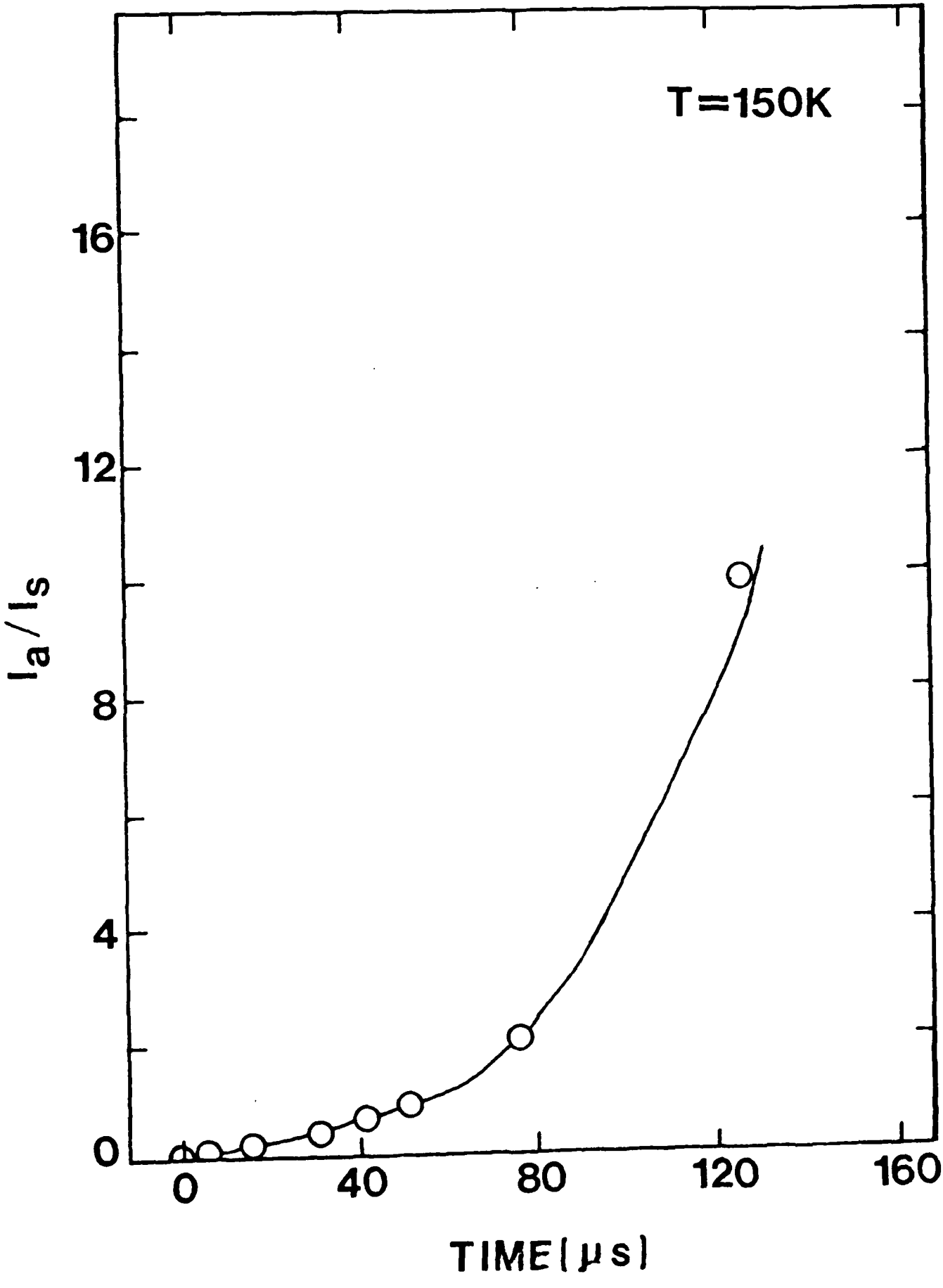
T=150K
16
12
8
4
0
I_a/I_s
0
40
80
120
160
TIME[μs]

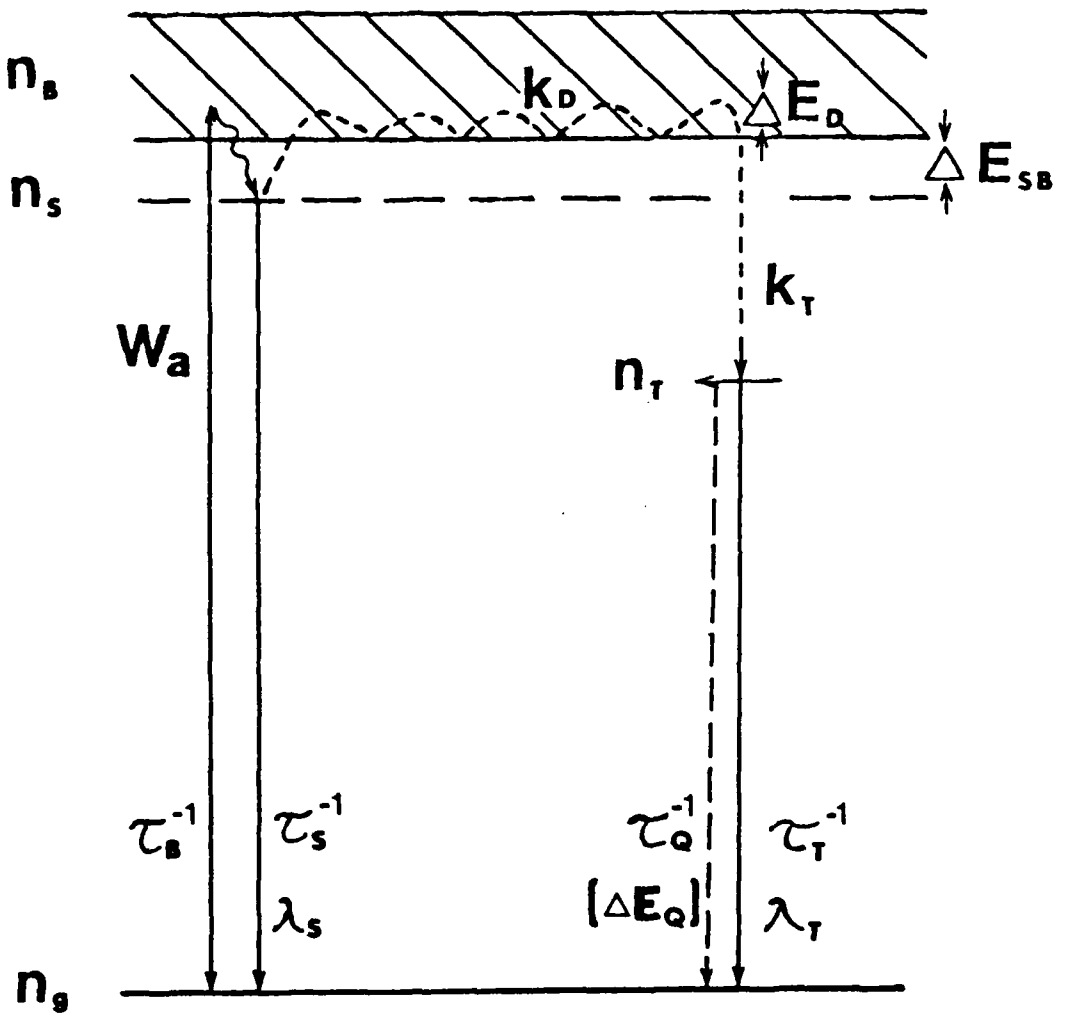
n_B
k_D
E_D
E_{SB}
n_S
k_T
W_a
n_T
τ_B^{-1}
τ_S^{-1}
τ_Q^{-1}
τ_T^{-1}
λ_S
$[\Delta E_Q]$
λ_T
n_g

END

FILMED

6-85

DTIC